

ARTICLE OPEN



SIRT1 ISGylation accelerates tumor progression by unleashing SIRT1 from the inactive state to promote its deacetylase activity

Ji An Kang^{1,2,3,13}, Yoon Jung Kim^{1,2,3,13}, Kyu Yun Jang⁴, Hye Won Moon^{1,3}, Haeseung Lee⁵, Seonjeong Lee^{6,7}, Hyun Kyu Song⁸, Sang Woo Cho⁹, Yoon Sun Yoo^{1,3}, Hye Gyeong Han^{1,3}, Min-Ju Kim⁵, Myoung Ja Chung⁴, Cheol Yong Choi⁹, Cheolju Lee^{6,7}, Chaeuk Chung¹⁰, Gang Min Hur¹¹, You-Sun Kim¹² and Young Joo Jeon^{1,3}✉

© The Author(s) 2024

ISG15 is an interferon-stimulated ubiquitin-like protein (UBL) with multifaceted roles as a posttranslational modifier in ISG15 conjugation (ISGylation). However, the mechanistic consequences of ISGylation in cancer have not been fully elucidated, largely due to a lack of knowledge on the ISG15 target repertoire. Here, we identified SIRT1, a nicotinamide adenine dinucleotide (NAD⁺)-dependent protein deacetylase, as a new target for ISGylation. SIRT1 ISGylation impairs the association of SIRT1 with its negative regulator, deleted in breast cancer 1 (DBC1), which unleashes SIRT1 from its inactive state and leads to an increase in its deacetylase activity. Importantly, SIRT1 ISGylation promoted lung cancer progression and limited lung cancer cell sensitivity to DNA damage-based therapeutics in vivo and in vitro models. The levels of ISG15 mRNA and protein were significantly higher in lung cancer tissues than in adjacent normal tissues. Accordingly, elevated expression of SIRT1 and ISG15 was associated with poor prognosis in lung cancer patients, a finding that could be translated for lung cancer patient stratification and disease outcome evaluation. Taken together, our findings provide a mechanistic understanding of the regulatory effect of SIRT1 ISGylation on tumor progression and therapeutic efficacy in lung cancer.

Experimental & Molecular Medicine (2024) 56:656–673; <https://doi.org/10.1038/s12276-024-01194-2>

INTRODUCTION

Interferon (IFN)-stimulated gene 15 (ISG15), the first identified ubiquitin-like protein (UBL), is highly expressed in many tumor types^{1,2}. ISG15 functions in tumor development, tumor aggressiveness, cell self-renewal, and cell-to-cell communication in the tumor microenvironment^{3–8}, suggesting that ISG15 is an active player in cancer pathogenesis rather than a passive observer. ISG15 exists in three distinct forms: unconjugated within the cell, conjugated to target proteins within the cell, and released into the extracellular space^{9–11}. In a similar manner to ubiquitination, the conjugation of ISG15 to target proteins (ISGylation) is accomplished through a three-step enzymatic cascade involving E1 activating, E2 conjugating, and E3 ligase enzymes, and the reversal of ISGylation is accomplished by ubiquitin-specific protease 18 (USP18)^{12–22}. Unlike the constitutive expression of some UBLs, ISG15 and the enzymes that catalyze ISGylation are robustly induced by IFNs, viral and bacterial infection, or genotoxic stresses^{2,12,21,23–27}, indicating that ISGylation is a tightly fine-tuned process modulated by various physiological and

pathophysiological perturbations. To comprehensively identify the targets of ISGylation, i.e., the “ISGylome”, numerous quantitative proteomics analyses have been performed^{28–32}, and the results demonstrated that targets of ISGylation are associated with various signaling pathways in a cell- and tissue type-dependent manner. However, obtaining a mechanistic understanding of how ISGylation modulates cell proliferation and therapeutic efficacy in cancer is complicated due to the need to consider the specific tumor context. We previously reported that ΔNp63α ISGylation modulates epithelial tumor progression²³. We found that ultraviolet-induced PCNA ISGylation is involved in the maintenance of genome stability²⁵. Furthermore, we demonstrated that p53 ISGylation regulates its transactivity³³. Our previous findings have therefore contributed to delineating the important roles of ISGylation in the control of cancer pathogenesis and the therapeutic response.

SIRT1 is a class III histone deacetylase that uses nicotinamide adenine dinucleotide (NAD⁺) as a cosubstrate for its enzymatic activity and deacetylates histone and nonhistone substrates,

¹Department of Biochemistry, Chungnam National University College of Medicine, Daejeon 35015, Republic of Korea. ²Brain Korea 21 FOUR Project for Medical Science, Chungnam National University, Daejeon 35015, Republic of Korea. ³Department of Medical Science, Chungnam National University College of Medicine, Daejeon 35015, Republic of Korea. ⁴Department of Pathology, Jeonbuk National University Medical School, Research Institute of Clinical Medicine of Jeonbuk National University-Biomedical Research Institute of Jeonbuk National University Hospital and Research Institute for Endocrine Sciences, Jeonju 54896, Republic of Korea. ⁵College of Pharmacy, Pusan National University, Busan 46241, Republic of Korea. ⁶Chemical & Biological Integrative Research Center, Korea Institute of Science and Technology, Seoul 02792, Republic of Korea. ⁷Division of Bio-Medical Science & Technology, KIST School, University of Science and Technology, Seoul 02792, Republic of Korea. ⁸Department of Life Sciences, Korea University, Seoul 02841, Republic of Korea. ⁹Department of Biological Sciences, Sungkyunkwan University, Suwon 16419, Republic of Korea. ¹⁰Division of Pulmonology and Critical Care Medicine, Department of Internal Medicine, College of Medicine, Chungnam National University, Daejeon 34134, Republic of Korea. ¹¹Department of Pharmacology, Chungnam National University College of Medicine, Daejeon 35015, Republic of Korea. ¹²Department of Biochemistry, Ajou University, School of Medicine & Department of Biomedical Sciences, Graduate School, Ajou University, Suwon 16499, Republic of Korea. ¹³These authors contributed equally: Ji An Kang, Yoon Jung Kim. ✉email: yjjeon@cnu.ac.kr

Received: 24 May 2023 Revised: 29 November 2023 Accepted: 26 December 2023

Published online: 5 March 2024

serving as a crucial link connecting multiple biological activities, including metabolism, inflammation, lifespan prolongation, and aging³⁴. Importantly, SIRT1 is involved in tumor progression and the therapeutic response³⁵. Furthermore, accumulating evidence indicates that SIRT1 activity is tightly modulated in response to multiple stresses³⁶. Therefore, understanding the regulatory mechanism of SIRT1 in distinct contexts is highly important and could contribute to therapeutic interventions for cancer.

Here, we identified SIRT1 as a new target for ISGylation. SIRT1 ISGylation impairs the association of SIRT1 with its negative regulator, deleted in breast cancer 1 (DBC1), which unleashes SIRT1 from its inactive state and leads to an increase in its deacetylase activity. Accordingly, SIRT1 ISGylation promoted lung cancer progression and limited lung cancer cell sensitivity to DNA damage-based therapeutics in *in vivo* and *in vitro* models, and elevated expression of SIRT1 and ISG15 was associated with poor prognosis in lung cancer patients. Taken together, our findings provide a deep understanding of the molecular mechanism of SIRT1 ISGylation to determine its contribution to tumor progression and the response to therapy.

MATERIALS AND METHODS

Plasmids, shRNAs, and siRNAs

The Flag-ISG15, Flag-USP18, Myc-UbcH8, UBE1L, and Myc-DBC1 expression plasmids have been described previously^{23,25}. Human SIRT1 cDNA and its deletion mutants were cloned into pcDNA4-HisMax (V864-20, Thermo Fisher Scientific, Waltham, MA, USA). The SIRT1-V5 (HsCD00871341) and AROS-V5 (HsCD00442690) expression plasmids were purchased from the Arizona State University (ASU) Biodesign Institute (Tempe, AZ, USA). Human AROS cDNA was cloned into pcDNA4-HisMax (V864-20, Thermo Fisher Scientific). Human ISG15 (M-004235-04-0010) and DBC1 (M-010427-01-0005) siGENOME SMARTpools and siGENOME nontargeting small interfering RNA (D-001206-14-20) were purchased from Dharmacon, a Horizon Discovery Group Co. (Cambridge, UK). sgControl-lentiCRISPRv2 (107402) was purchased from Addgene (Watertown, MA, USA).

CRISPR–Cas9-mediated genome editing

The SIRT1 KO cell line was generated by CRISPR–Cas9-mediated genome editing. In brief, annealed oligonucleotides containing the gRNA target sequence (5'-CTCCGCAAGAGGCCGCGAG-3') were cloned into the lentiCRISPRv2 vector. The lentiCRISPRv2 vector containing the sgRNA against SIRT1 or sgControl was transfected into HEK293T cells along with the Gag-Pol (pCMV Δ8.91 R) and VSV-G (pMD-G) plasmids. Lentiviral particles were collected 48 h after transfection. A549 cells were transduced by incubation with the viral supernatant (1.5 ml), fresh medium (8.5 ml), and polybrene (7.5 µg/ml). After 24 h, the transduced cells were maintained in DMEM supplemented with 2 µg/ml puromycin. Typical colonies were picked from the plates using cloning cylinders, subcultured, and expanded. SIRT1 KO clonal cell lines were characterized using genomic DNA sequencing, immunocytochemistry, and immunoblotting with an anti-SIRT1 antibody.

Lentivirus production and lentiviral transduction of SIRT1 KO A549 cells

To stably re-express SIRT1 in the SIRT1 KO clonal cell line, we used a lentiviral vector expressing the SIRT1 sgRNA-resistant SIRT1-V5 (HsCD00871341, ASU Biodesign Institute) or a lentiviral control vector (40125, Addgene). Lentiviruses were produced by transfecting a lentiviral vector and HIV packaging mix (LT002-01, GeneCopoeia, Rockville, MD, USA) into HEK293FT cells (R70007, Thermo Fisher Scientific) using Lipofectamine 2000 (11668027, Thermo Fisher Scientific). Lentiviral particles were collected 72 h after transfection. SIRT1 KO cells were then transduced with lentivirus in the presence of 10 µg/ml polybrene. After 36 h, the transduced cells were maintained in DMEM supplemented with 10 µg/ml blasticidin. Typical colonies were picked from the plates using cloning cylinders, subcultured, and expanded.

Antibodies and chemicals

Antibodies against SIRT1 (5322, Sigma–Aldrich, St. Louis, MO, USA; sc-15404, Santa Cruz, Dallas, TX, USA; or 07-131, Millipore, Temecula, CA, USA), ISG15 (15981-1-AP, Proteintech, Rosemont, IL, USA; or HPA004627, Atlas

Antibodies, Bromma, Sweden), Ac-p53 (2525, Cell Signaling, Danvers, MA, USA), phospho-p53 (9284, Cell Signaling), p53 (sc-126, Santa Cruz), DBC1 (A300-434A, Bethyl Laboratories, Montgomery, TX, USA), cleaved PARP (9541, Cell Signaling), Xpress (R910-25, Thermo Fisher Scientific), Flag M2 (F1804, Sigma–Aldrich), V5 (R960-25, Thermo Fisher Scientific), c-Myc (C3946, Sigma–Aldrich; or sc-40, Santa Cruz), β-actin (sc-47778, Santa Cruz), and GAPDH (MA5-15738, Invitrogen, Waltham, MA, USA) were used. Anti-V5 agarose affinity gel was purchased from Sigma–Aldrich (A7345). Doxorubicin (D1515), camptothecin (S1288), cisplatin (S1166), and recombinant human IFN-α A (α 2a) (11100-1) were purchased from Sigma–Aldrich, Selleckchem (Houston, TX, USA), Selleckchem, and R&D Systems (Minneapolis, MN, USA), respectively.

Cell culture and transfection

HEK293T, HEK293FT, C-33A, HeLa, A549, MCF7, Huh7 and HepG2 cells were maintained at 37 °C in a 5% CO₂ atmosphere in DMEM (Welgene, Daegu, Korea) supplemented with 10% FBS (Gibco, Thermo Fisher, Waltham, MA, USA). H23 and T47D cells were cultured at 37 °C in a 5% CO₂ atmosphere in RPMI 1640 (Welgene, Daegu, Korea) supplemented with 10% FBS. Transfection was performed using jetPRIME (114-75, Polyplus, Illkirch-Graffenstaden, FR), DharmaFECT1 (T-2001-03, Dharmacon) or Lipofectamine RNAiMAX (13778-150, Thermo Fisher Scientific).

Immunoprecipitation and NTA pulldown

Cells were lysed in 50 mM Tris-HCl (pH 8) supplemented with 150 mM NaCl, 0.5% NP-40, 1 mM PMSF, and 1X protease inhibitor cocktail (11 697 498 001, Roche Applied Science, Basel, Switzerland) in the absence or presence of 0.25% SDS. The cell lysates were incubated with appropriate antibodies for 3 h at 4 °C, after which 20 µl of protein A/G agarose beads was added (sc-2003, Santa Cruz) and the mixture was incubated for an additional 2 h. For pulldown with NTA resin, cells were lysed in 50 mM Tris-HCl (pH 8) supplemented with 150 mM NaCl, 10 mM imidazole, 0.5% NP-40, 1 mM PMSF, and 1X protease inhibitor cocktail. The cell lysates were incubated with NTA resin (25215, Thermo Fisher Scientific) for 3 h at 4 °C. Harvested xenograft tumors were lysed in 50 mM Tris-HCl (pH 8) supplemented with 150 mM NaCl, 0.5% NP-40, 1 mM PMSF, and 1X protease inhibitor cocktail (11 697 498 001, Roche Applied Science) by using an ultrasonic homogenizer. The tumor lysates were incubated with appropriate antibodies for 3 h at 4 °C, after which 20 µl of protein A/G agarose beads was added (sc-2003, Santa Cruz) and the mixture was incubated for an additional 2 h.

ISGylation sites mapping by mass spectrometry

V5-tagged SIRT1 WT was expressed in HEK293T cells in the presence of the ISG15-conjugating system and then purified via immunoprecipitation with an anti-V5 antibody. Proteins in the immunoprecipitates were separated by SDS–PAGE and visualized by staining with Coomassie blue R250. The Coomassie-stained gel was rinsed with water. The gel spot that was shifted upward from the position of main SIRT1 band was excised and chopped into smaller pieces. These gel pieces were destained with 100 mM ammonium bicarbonate/acetonitrile (1:1, v/v). In-gel digestion with trypsin was then performed as previously described³⁷. LC–MS/MS analysis of the peptides extracted from the gel was performed on a Q Exactive mass spectrometer coupled to an UltiMate 3000 HPLC system (Thermo Fisher Scientific). In this LC–MS system, the peptides were separated on an EASY-Spray column (15 cm × 75 µm I.D., C18, particle size of 2 µm, Thermo Fisher Scientific). Mobile phases A and B were 0.1% (v/v) formic acid and 0.1% (v/v) formic acid in 80% (v/v) acetonitrile, respectively. Peptides were eluted with a linear gradient from 2% to 40% buffer B over 55 min at a flow rate of 300 nL/min. The parameters for mass spectrometry were set as previously described³⁸.

Mass spectra were analyzed with the SEQUEST HT module in Proteome Discoverer 2.4 (Thermo Fisher Scientific) and searched against the human proteome database downloaded from UniProt (20,591 entries, Release 2023_01). The mass tolerance values were set to 10 ppm and 0.02 Da for the precursor and the fragment ions, respectively. The search parameters were as follows: full tryptic specificity with up to two missed cleavages and cysteine carbamidomethylation (+57.021 Da) as the static modification. The variable modifications included methionine oxidation (+15.995 Da) and lysine GlyGly modification (+114.043 Da). The false discovery rate (FDR) was set to 0.01 both at the peptide and at the peptide spectrum match (PSM) levels with the Percolator module. The resultant spectra were further filtered based on the XCorr scores (≥1.9, 2.2, and 3.75 for precursor charge states of +1, +2, and +3 or higher, respectively). Annotated MS/MS

spectra were generated using the freely accessible web tool Interactive Peptide Spectrum Annotator (IPSA)³⁹.

SIRT1 activity assay

The deacetylase activity of SIRT1 was evaluated by using a SIRT1 Activity Assay Kit (ab156065, Abcam, Cambridge, UK) as recommended by the manufacturer. Briefly, cells were washed with cold PBS and lysed in 50 mM Tris-HCl (pH 8) supplemented with 150 mM NaCl and 0.5% NP-40 in the presence or absence of 10 mM imidazole. Cell lysates were subjected to pulldown with NTA resin (25215, Thermo Fisher Scientific) for 3 h at 4 °C or incubated with an anti-SIRT1 antibody for 3 h at 4 °C. Afterward, 20 µl of protein A/G agarose beads was added (sc-2003, Santa Cruz), and the mixture was incubated for an additional 2 h. The precipitates were incubated with Fluoro-Substrate Peptide Solution, NAD⁺, and SIRT1 assay buffer. The fluorescence intensity was subsequently measured using a microtiter plate fluorometer with an excitation wavelength of 350 nm and an emission wavelength of 450 nm.

Cell growth and clonogenic assays

For the cell growth assay, cells (5×10^3) were seeded and incubated in triplicate for 24 h. The cells were then treated with 1 µM doxorubicin for 24 h before harvesting. Viable cells were counted following trypan blue staining. For the clonogenic assay, cells were plated in 6-well plates (400 cells in 2 ml of medium per well). The medium was not changed during the experiment. After 13 days, the colonies were fixed, stained with crystal violet, and counted.

TUNEL assay

Cells were cultured on glass coverslips. After incubation with 1 µM doxorubicin for the indicated times, the cells were fixed with 3.7% paraformaldehyde for 10 min and subjected to a terminal deoxynucleotidyl transferase-mediated dUTP-fluorescein nick end-labeling (TUNEL) assay with an in situ cell death detection kit following the manufacturer's instructions (11684795910, Roche Applied Science).

Animal studies

All animal experiments were approved by the Institutional Animal Care and Use Committee (IACUC) of Chungnam National University (Approval number: CNUH-020-A0020-1). Animal care was conducted according to institutional guidelines. SIRT1 KO A549 cells (7.5×10^6) stably expressing empty vector, SIRT1 WT or SIRT1 KR were subcutaneously injected into the flanks of 6-week-old BALB/c nude mice. On the fourth day after injection, the mice were randomly allocated into different treatment groups (6 mice per group) and received intraperitoneal injections of PBS or doxorubicin (1.25 mg/kg) twice weekly for 5 weeks. The mice were monitored regularly for tumor growth. Tumor volumes were calculated as $(a \times a \times b)/2$, where a is the smallest diameter and b is the largest. At the end of the experiments, the mice were sacrificed, and the tumors were harvested.

Lung cancer patients and tissue samples

Tumor and adjacent normal tissues obtained from adenocarcinoma lung cancer patients were provided by the Human Resources Bank of Chungnam National University Hospital (IRB number CNUH 2021-06-007). A cohort of lung cancer patients ($n = 89$, patients diagnosed between 2011 and 2012) was generated and represented patients diagnosed at Chonbuk National University Hospital. All cases were reviewed according to the WHO classification and the American Joint Committee Cancer Staging System. Information on clinicopathological factors was obtained by a review of medical records. All the samples were obtained with the approval of the Institutional Review Board of Chonbuk National University Hospital (IRB number CUH 2018-10-026-001). Analysis was performed in accordance with the tenets of the Declaration of Helsinki.

Immunohistochemical staining and scoring

Dual-immunohistochemical staining for SIRT1 and ISG15 was performed using a Ventana BenchMark ULTRA system (Roche Korea Diagnostics Ltd., Seoul, Korea). Antigen retrieval was performed for 64 min using pH 9.0 CC1 antigen retrieval solution (Roche Korea Diagnostics Ltd.). The specimens were incubated with primary antibodies (anti-SIRT1 (sc-15404), 1:100, Santa Cruz; and anti-ISG15 (HPA004627), 1:100, Atlas Antibodies) for 90 min, and developed with an OptiView DAB IHC Detection Kit (Roche Korea Diagnostics Ltd.) for SIRT1 and with an UltraView Universal Alkaline

Phosphatase Red Detection Kit (Roche Korea Diagnostics Ltd.) for ISG15. For quantification, the combined expression of SIRT1 and ISG15 (SIRT1/ISG15) and the individual expression of SIRT1 or ISG15 were assessed. The combined expression of SIRT1 and ISG15 (SIRT1/ISG15) and the individual expression of SIRT1 or ISG15 were scored by summing the staining intensity score (0; no staining, 1; weak staining, 2; intermediate staining, 3; strong staining) and the area score (0; 0%, 1; 1%, 2; 2–10%, 3; 11–33%, 4; 34–66%, 5; 67–100%)⁴⁰. The final score was assessed by summing the scores from the two tissue microarray cores, resulting in a final immunohistochemical staining score ranging from zero to sixteen⁴¹.

Analysis of lung cancer patients

The cutoff points for the scores for the combined expression of SIRT1 and ISG15 (SIRT1/ISG15) and the individual expression of SIRT1 or ISG15 were determined by receiver operating characteristic curve analysis. The cutoff points were determined as the points with the greatest area under the curve for predicting the death of lung cancer patients. Survival analysis was also performed to evaluate the overall survival of patients. The death of a lung cancer patient was considered a death event. Patients who were alive at last contact or who died from other causes were considered censored. To determine the relationships between clinicopathological factors and the prognostic impact of survival factors, Pearson's chi-square test, univariate and multivariate Cox proportional hazards regression analyses, and Kaplan–Meier survival analysis were performed using SPSS software (IBM, version 20.0, CA). $P < 0.05$ was considered to indicate statistical significance.

Statistical analysis

The sample size and statistical significance of differences are described in the figure legends. All the quantitative data are presented as the mean \pm SD or \pm SEM of at least three independent experiments as determined by Student's t test for between-group differences. $P < 0.05$ was considered to indicate statistical significance.

Ethics approval

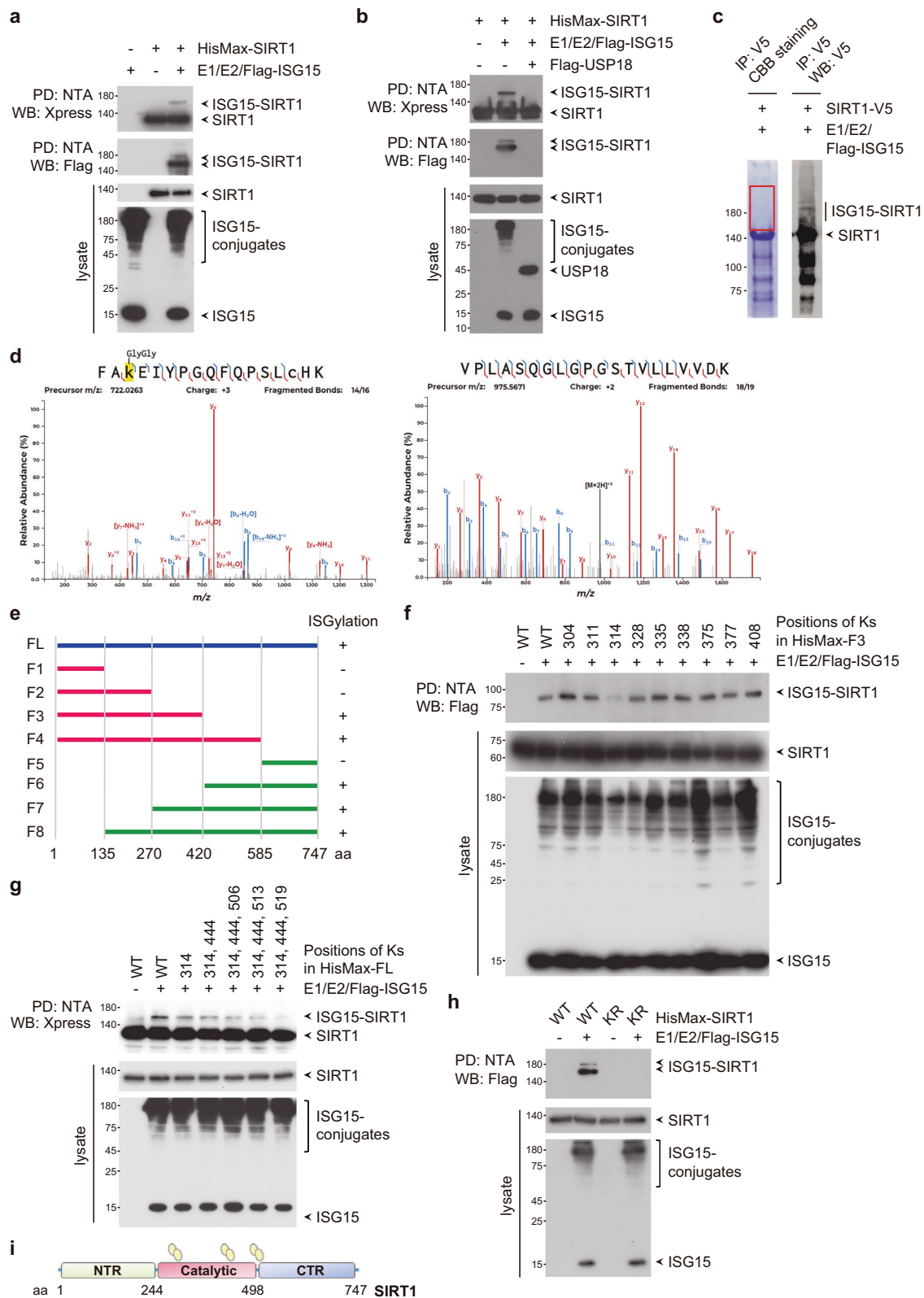
Lung cancer patient samples were obtained with the approval of the Institutional Review Board of Chonbuk National University Hospital (IRB number CUH 2018-10-026-001) or Chungnam National University Hospital (IRB number CNUH 2021-06-007). All animal experiments were approved by the Institutional Animal Care and Use Committee (IACUC) of Chungnam National University (Approval number: CNUH-020-A0020-1). Animal care was conducted according to institutional guidelines.

RESULTS

SIRT1 is ISGylated

To elucidate the mechanisms of action of ISG15 in cancer, we utilized a proteomic approach and analyzed proteins retrieved from HEK293T cells expressing the E1 activating enzyme UBE1L, the E2 conjugating enzyme UbcH8, and Flag-tagged ISG15 (collectively henceforth referred to as the ISG15-conjugating system) by immunoaffinity purification using anti-Flag antibody-immobilized resin. Among the putative targets for ISGylation (Supplementary Fig. 1), we selected SIRT1, as SIRT1 has been suggested to impact cancer pathogenesis. To verify whether SIRT1 is ISGylated, we coexpressed SIRT1 with the ISG15-conjugating system. Overexpression of SIRT1 with the ISG15-conjugating system led to the appearance of at least two ISGylated SIRT1 bands (Fig. 1a). Moreover, these bands disappeared upon coexpression of USP18, a major deISGylating enzyme (Fig. 1b), indicating that the bands correspond to ISGylated SIRT1.

To determine which lysine residues are critical for SIRT1 ISGylation, we performed mass spectrometry (MS) on SIRT1-V5 purified from HEK293T cells coexpressing SIRT1 and the ISG15-conjugating system. Coomassie blue R250-stained bands corresponding to ISGylated SIRT1 were excised for MS analysis (Fig. 1c). SIRT1 was identified with 72% sequence coverage (Supplementary Fig. 2). Among the identified peptides matched to SIRT1, two were found to be GlyGly modified (Fig. 1d, left and Supplementary Fig. 3) at Lys (K) 314 and K513 (highlighted in red in



Supplementary Fig. 2). The GlyGly motif is from ISG15, as ISG15 was also identified in the same gel band (Fig. 1d, right and Supplementary Fig. 4). GlyGly modification results in the retention of the last two amino acid residues of ISG15 at SIRT1 after trypsin digestion. The GlyGly modified K314 peptide had more peptide

spectral matches (PSMs) than did the corresponding K513 peptide. Using a label-free quantification (LFQ) approach, we compared the signal intensities of not only the GlyGly-modified K314 and K513 peptides but also the unmodified K314 and K513 peptides, assumed to have the amino acid sequences EIYPGQFQPSLCHK

Fig. 1 SIRT1 is a novel target for ISGylation. HisMax-SIRT1 or the ISG15-conjugating system (E1/E2/Flag-ISG15) were overexpressed alone or in combination in HEK293T cells without (a) and with (b) Flag-USP18 expression. Cell lysates were subjected to pulldown (PD) with NTA resin followed by Western blotting (WB) with an anti-Flag or anti-Xpress antibody. The lysates were also directly probed with the same antibodies. c Coomassie blue R250-stained gel showing enrichment of SIRT1-V5 immunoprecipitated from HEK293T cells. Coomassie blue R250-stained bands corresponding to ISGylated SIRT1-V5 were excised for MS/MS. Five percent of the SIRT1-V5-enriched immunoprecipitate was subjected to WB analysis with an anti-V5 antibody. d (Left) Annotated MS/MS spectrum of the peptide FAKEIYPGQFQPSLCHK from the SIRT1 protein. The Lys residue, highlighted in yellow, is at position 314 in the SIRT1 protein and is GlyGly modified (+114.042927 Da). The Cys residue of the peptide, indicated in lower case text, is carbamidomethylated (+57.021464 Da). (Right) Annotated MS/MS spectrum of the peptide VPLASQGLGPGSTVLLVVDK from the ISG15 protein. e Deletion mutants of HisMax-SIRT1 were generated. Whether each deletion was modified by ISG15 is indicated on the right. FL full-length. F fragment. HisMax-tagged F3 (f), FL SIRT1 and K-to-R mutants in various combinations (g) and SIRT1 WT or SIRT1 KR (h) were expressed in HEK293T cells along with the ISG15-conjugating system. Cell lysates were subjected to PD with NTA resin followed by WB with an anti-Xpress or anti-Flag antibody. i Domain structures of SIRT1. The ISGylation sites Lys314, Lys444, and Lys519 are denoted. NTR N-terminal regulatory domain, Catalytic catalytic core domain, CTR C-terminal regulatory domain.

and LSEITEKPPR, respectively. The signal intensity of the GlyGly-modified K314 peptide was 5-fold greater than that of the GlyGly-modified K513 peptide, while the signal intensities of the peptides with unmodified K314 or K513 residues were similar (Supplementary Fig. 5), suggesting that K314 is the major potential site of ISGylation.

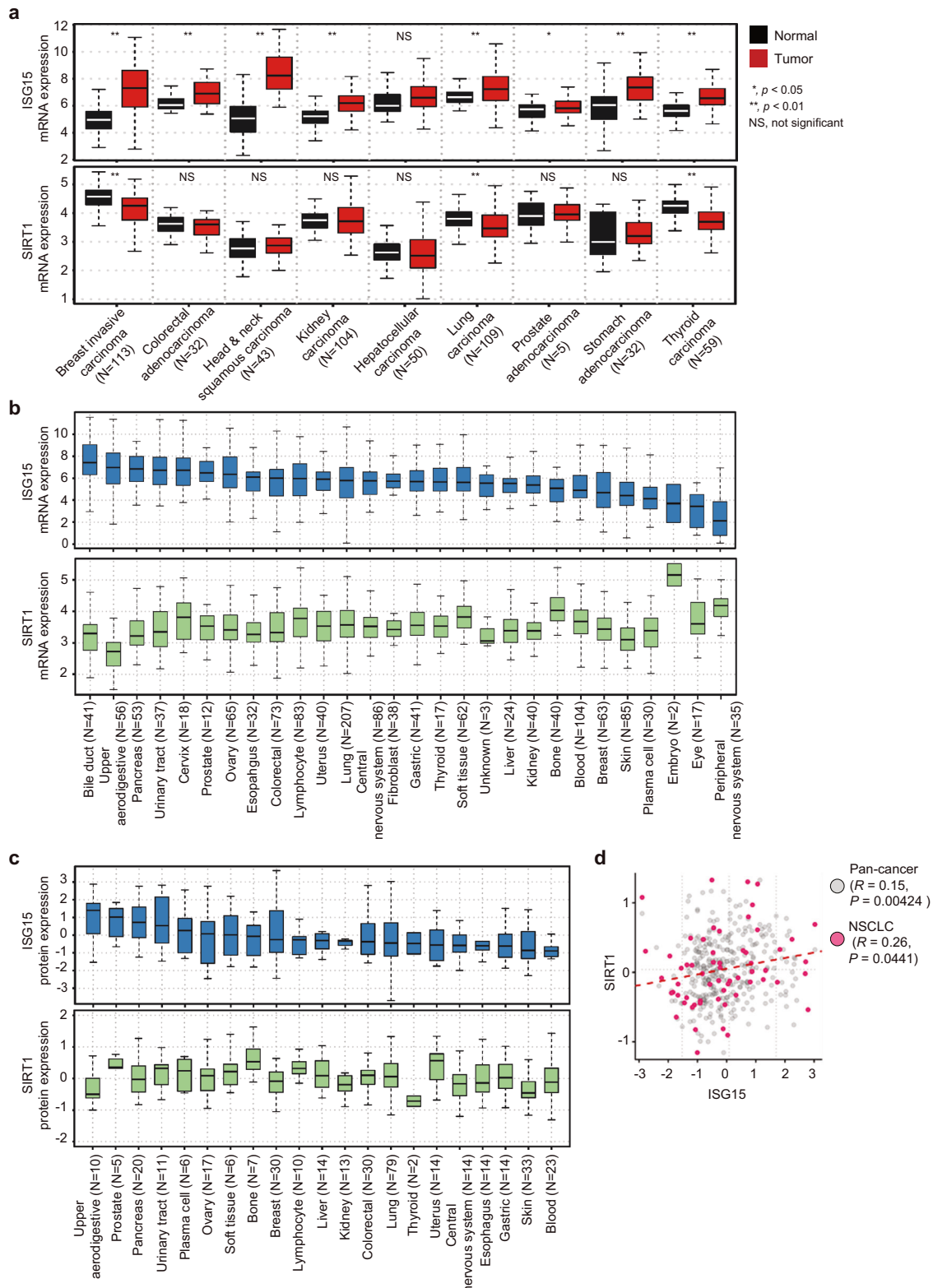
To further determine which lysine residues in SIRT1 are ISGylated, various deletion mutants of SIRT1 (termed fragment (F)1 to F8) were generated and expressed in HEK293T cells along with the ISG15-conjugating system. Full-length SIRT1 (FL; i.e., containing aa 1-747), F3 (containing aa 1-420), F4 (containing aa 1-585), F6 (containing aa 421-747), F7 (containing aa 271-747), and F8 (containing aa 136-747) but not F1 (containing aa 1-135), F2 (containing aa 1-270), or F5 (containing aa 586-747) were conjugated by ISG15, indicating that the deletion mutants containing aa 271-420 and aa 421-585 had ISGylation sites (Fig. 1e). In accordance with the results of our MS analysis (Fig. 1d), among the 9 Lys residues in the aa 271-420 sequence within F3, the substitution of Lys314 with arginine (Arg) but no other Lys (K)-to-Arg (R) substitutions noticeably reduced the ISGylation of F3 (Fig. 1f). Since the deletion mutants containing aa 421-585 also have ISGylation sites (Fig. 1e), we next replaced 10 Lys residues in the aa 420-585 sequence with Arg in full-length SIRT1 (FL) harboring the K314R substitution. Full-length SIRT1 harboring the K314R/K444R, K314R/K506R, K314R/K513R or K314R/K519R double substitution showed markedly diminished ISGylation (Supplementary Fig. 6). We, therefore, replaced Lys residues with Arg residues in full-length SIRT1 in various combinations. Notably, relative to the K314R/K444R/K513R triple substitution, the K314R/K444R/K519R triple substitution in SIRT1 (referred to herein as SIRT1 KR) almost completely abolished the ISGylation of SIRT1, even though K513 was identified as a putative site of ISGylation in the MS analysis (Fig. 1g, h). Considering the result of these analyses collectively, we suggest that Lys314 within the catalytic core domain is a major ISGylation site and that Lys444 within the catalytic core domain and Lys519 within the C-terminal extension are minor ISGylation sites in SIRT1 (Fig. 1i).

Given that the contributions of ISG15 and SIRT1 to cancer pathogenesis are complex and remain elusive, we analyzed the mRNA and protein expression levels of ISG15 and SIRT1 in The Cancer Genome Atlas (TCGA) and the Cancer Cell Line Encyclopedia (CCLE) database^{42,43}. We first analyzed data from the TCGA database to compare the *ISG15* mRNA level among tumor tissues and adjacent normal tissues from patients with nine types of cancer. This analysis revealed that the *ISG15* mRNA level was significantly higher in all tumor tissues except for hepatocellular carcinoma tissues than in the corresponding adjacent normal tissues (Fig. 2a, upper). Our results are consistent with previous reports demonstrating the upregulation of ISG15 in several types of cancer^{3,44–48} and suggest that ISG15 is directly or indirectly involved in cancer development. However, the *SIRT1* mRNA level was not significantly different between the tumor and adjacent normal tissues in any cancers examined, except for invasive breast,

lung, and thyroid carcinomas, in which the *SIRT1* mRNA level was significantly lower in the tumor tissues than in the adjacent normal tissues (Fig. 2a, lower). Further analyses of RNA sequencing (RNA-Seq) data from 1404 cancer cell lines across 28 cancer types and proteomic data from 375 cancer cell lines across 21 cancer types from the CCLE database revealed similar mRNAs and protein expression levels of ISG15 and SIRT1 in various cancer cell lines (Fig. 2b, c). Interestingly, the protein expression level of ISG15 showed a subtle yet significant positive correlation with the protein expression level of SIRT1 in the complete set of cancer types ($R = 0.15$, $P = 0.0042$) as well as in non-small cell lung carcinoma (NSCLC) ($R = 0.26$, $P = 0.0441$) (Fig. 2d).

In contrast to the constitutive expression of some UBLs, the expression of ISG15 and the enzymes that catalyze ISGylation is strongly induced by physiological and pathophysiological perturbations. Moreover, we previously reported that doxorubicin, a DNA-damaging chemotherapeutic, robustly induces ISG15 expression and the formation of protein ISGylation conjugates^{23,25,33}. Therefore, we determined whether doxorubicin induces ISG15 expression and the formation of protein ISGylation conjugates in cell lines derived from lung, cervical, breast or liver cancer. Significant induction of both ISG15 expression and protein ISGylation conjugates formation in the presence of doxorubicin was observed in A549 and H23 cells derived from lung cancer and in HeLa cells derived from cervical cancer (Fig. 3a). However, doxorubicin treatment had little or no effect on the induction of ISG15 expression and protein ISGylation conjugates formation in C33A cells derived from cervical cancer. Liver cancer-derived HepG2 cells but not Huh7 cells exhibited moderate induction of both ISG15 expression and protein ISGylation conjugates formation. MCF7 and T47D cells derived from breast cancer showed weak induction of ISG15 expression and protein ISGylation conjugates formation, even though protein ISGylation conjugates were present even in the absence of doxorubicin. We further investigated whether doxorubicin induces SIRT1 ISGylation in cell lines derived from lung, cervical, breast or liver cancer. Doxorubicin induced ISGylation of endogenous SIRT1 in both A549 and H23 cells derived from lung cancer, in which it was robustly able to induce ISG15 expression and protein ISGylation conjugates formation (Fig. 3b). Furthermore, HeLa cells derived from cervical cancer and MCF7 cells derived from breast cancer showed significant evidence of SIRT1 ISGylation upon doxorubicin treatment (Supplementary Fig. 7), suggesting that SIRT1 is a bona fide target for ISGylation in a subset of cancer cells. Intriguingly, SIRT1 has been reported to play an important role in lung cancer development and chemoresistance⁴⁹. Therefore, these findings prompted us to focus on lung cancer to explore the role of SIRT1 ISGylation in cancer pathogenesis. However, further studies might be required to expand the understanding of SIRT1 ISGylation in various cancers.

DNA-damaging chemotherapeutics reportedly upregulate ISGylation²³. For example, camptothecin increases the levels of free ISG15 and its conjugates in a dose- and time-dependent manner⁵⁰. We therefore examined whether other chemotherapeutic drugs, i.e.,



camptothecin and cisplatin, induce ISG15 expression and protein ISGylation conjugates formation. In A549 cells, camptothecin treatment induced ISG15 expression and protein ISGylation conjugates formation, whereas cisplatin treatment had little or no effect on the induction of ISG15 expression and protein ISGylation conjugates formation (Fig. 3c, d). Accordingly, camptothecin but not cisplatin induced the ISGylation of endogenous SIRT1 (Fig. 3d).

Type I IFNs activate the expression of hundreds of ISGs and regulate tumorigenesis through both tumor cell-intrinsic and tumor cell-extrinsic mechanisms, leading to tumor progression or tumor suppression in a context-dependent manner^{8,51,52}. ISG15 and the enzymes that catalyze ISGylation are robustly induced by type I IFNs. Hypoxia-inducible factor-1 α (HIF-1 α) has been reported to be ISGylated upon IFN treatment, which reduces the

Fig. 2 **ISG15 is upregulated in several types of cancer.** **a** mRNA expression levels of *ISG15* and *SIRT1* in paired tumor and adjacent normal tissues of nine tumor types in The Cancer Genome Atlas (TCGA) database. The TCGA RNA-seq data were obtained from the Genomic Data Commons (GDC), and log2-transformed transcripts per million (TPM) values are shown. **b** Boxplot showing the distribution of *ISG15* and *SIRT1* mRNA expression levels in 1404 cancer cell lines across 28 cancer types. mRNA expression values are presented as log2-transformed TPM values determined by RNA-seq using a pseudocount of 1. **c** Distribution of *ISG15* and *SIRT1* protein expression levels quantified by mass spectrometry in 375 cancer cell lines across 21 cancer types. Protein expression values are presented in a log2-transformed, normalized format. Proteomic and RNA-seq datasets of the cancer cell lines in the CCLE were obtained from the DepMap portal (<https://depmap.org/portal/>). **d** A scatter plot illustrating the relationship between *ISG15* and *SIRT1* protein expression across 375 cancer cell lines (depicted as gray dots) and 60 non-small cell lung carcinoma (NSCLC) cell lines (highlighted in red dots). The Pearson correlation coefficient (R) and the statistical significance of the correlation (P) were determined via a correlation test implemented in R software.

transcriptional activity of HIF-1 α and subsequently affects tumor growth⁵³. The type I IFN-mediated ISG–ISGylation network in the tumor microenvironment of breast cancer synergistically induces the expression of chemokine receptor ligands and attracts cytotoxic T cells, thereby orchestrating the establishment of a tumor-suppressive microenvironment⁸. In contrast, tumor cell resistance to type I IFNs has been demonstrated^{54–57}. Type I IFN-induced filamin B ISGylation acts as a negative feedback regulatory gate for the desensitization of IFN-induced JNK signaling and apoptosis⁵⁸. Parkin ISGylation induced by type I IFN promotes the ubiquitin E3 ligase activity of parkin, thereby increasing the protective effect of parkin against IFN-induced cell death⁵⁹, suggesting the double-edged roles of type I IFN-induced protein ISGylation in controlling tumor progression or tumor suppression. We investigated whether *SIRT1* can be ISGylated upon type I IFN treatment. *SIRT1* was weakly ISGylated upon IFN treatment compared with doxorubicin treatment, even though the IFN and doxorubicin induced *ISG15* expression and protein ISGylation conjugates formation to comparable degrees (Fig. 3e). A particular E2 conjugating or E3 ligase enzyme for *SIRT1* ISGylation might be differentially activated by different stimuli, suggesting that complex regulatory mechanisms may underlie ISGylation in a manner dependent on the biological context.

ISGylation enhances the deacetylase activity of *SIRT1*

To assess the molecular and functional consequences of ISGylation on *SIRT1*, we examined whether ISGylation affects the deacetylase activity of *SIRT1*. *SIRT1* WT or *SIRT1* KR was expressed in HEK293T cells in the absence or presence of the *ISG15*-conjugating system and was purified via pulldown with NTA resin (Supplementary Fig. 8a). The purified proteins were then subjected to an in vitro fluorometric assay to measure deacetylase activity. *SIRT1* WT showed a significant increase in deacetylase activity in the presence of the *ISG15*-conjugating system compared to in the absence of the *ISG15*-conjugating system (Fig. 4a). However, *SIRT1* KR showed no increase in deacetylase activity in the presence of the *ISG15*-conjugating system, suggesting that ISGylation substantially increases the deacetylase activity of *SIRT1*. To further improve the understanding of this phenomenon, we used CRISPR–Cas9 genome editing to ablate *SIRT1* and validated the expression of *SIRT1* in independent *SIRT1* knockout (*SIRT1* KO) A549 clonal cell lines via immunoblotting with an anti-*SIRT1* antibody (Supplementary Fig. 8b). Among the *SIRT1* KO clonal cell lines, we selected clone #2 and further verified the ablation of *SIRT1* using immunocytochemistry and genomic DNA sequencing analysis (Supplementary Fig. 8c, d). We also established sgControl- and lentiviral control vector-expressing A549 clonal cells (henceforth referred to as Control cells), two lentiviral control vector-expressing *SIRT1* KO cell lines, four *SIRT1* sgRNA-resistant *SIRT1* WT-complemented *SIRT1* KO clonal cell lines, and four *SIRT1* sgRNA-resistant *SIRT1* KR-complemented *SIRT1* KO clonal cell lines and validated the expression of *SIRT1* in these cell lines (Supplementary Fig. 8e). We selected clone #1 among the two lentiviral control vector-expressing *SIRT1* KO cell lines, clones #1 and #3 among the four *SIRT1* WT-complemented *SIRT1* KO cell lines, clones #1 and #4 among the four *SIRT1* KR-

complemented *SIRT1* KO cell lines, and Control cells and examined the protein levels of *SIRT1*, *ISG15* and ISGylation conjugates in the absence or presence of doxorubicin. Overall, the protein levels of *SIRT1*, *ISG15* and protein ISGylation conjugates were comparable among the clonal cell lines (Fig. 4b). Importantly, doxorubicin significantly induced *SIRT1* ISGylation in *SIRT1* WT-complemented *SIRT1* KO cells and Control cells but not in *SIRT1* KR-complemented *SIRT1* KO cells (Fig. 4b). Subsequently, clone #1 among the control vector-expressing *SIRT1* KO cell lines, clone #1 among the *SIRT1* WT-complemented cell lines, and clone #1 among the *SIRT1* KR-complemented cell lines were selected and referred to as *SIRT1* KO, *SIRT1* WT-complemented *SIRT1* KO, and *SIRT1* KR-complemented *SIRT1* KO cells, respectively. We expressed p53 in *SIRT1* KO, *SIRT1* WT-complemented and *SIRT1* KR-complemented *SIRT1* KO cells in the absence or presence of the *ISG15*-conjugating system. Consistent with the role of ISGylation in the deacetylase activity of *SIRT1*, deacetylation of p53 by *SIRT1* WT was potentiated compared to that by *SIRT1* KR in the presence of the *ISG15*-conjugating system (Supplementary Fig. 8f, g). In accordance with this finding, acetylation of endogenous p53 in the presence of doxorubicin was markedly increased in *SIRT1* KR-complemented *SIRT1* KO cells to a level approximately equal to that in *SIRT1* KO cells, while p53 acetylation in the presence of doxorubicin was only marginally increased in *SIRT1* WT-complemented *SIRT1* KO cells and Control cells (Fig. 4c).

Based on the substantial role of ISGylation in the deacetylase activity of *SIRT1*, we further examined the underlying mechanisms in more detail. DBC1, a tumor suppressor originally identified as a protein not expressed in breast cancer cells, binds to *SIRT1* and inhibits its enzymatic activity^{60,61}. We therefore hypothesized that *SIRT1* ISGylation might influence the interaction between *SIRT1* and its negative regulator DBC1. DBC1 and *SIRT1* WT or DBC1 and *SIRT1* KR were coexpressed in HEK293T cells in the absence or presence of the *ISG15*-conjugating system and were reciprocally coimmunoprecipitated using antibodies against Xpress or Myc. Coexpression of the *ISG15*-conjugating system strongly impaired the interaction of DBC1 with *SIRT1* WT but not with *SIRT1* KR (Fig. 4d, e), indicating that *SIRT1* ISGylation markedly promotes the dissociation of *SIRT1* from DBC1. To investigate whether doxorubicin-induced *SIRT1* ISGylation influences the physical interaction and functional connection between *SIRT1* and DBC1, we coimmunoprecipitated endogenous *SIRT1* and DBC1 from *ISG15* small interfering RNA (siRNA) (si*ISG15*)-expressing or siControl-expressing cells with and without doxorubicin treatment. Importantly, the interaction of *SIRT1* with DBC1 was attenuated following doxorubicin treatment in siControl-expressing cells (Fig. 4f). However, *ISG15* depletion led to the persistent association of *SIRT1* with DBC1 following doxorubicin treatment, suggesting that *SIRT1* ISGylation induced by doxorubicin negatively regulates the association of *SIRT1* with DBC1. We further examined whether doxorubicin-induced *SIRT1* ISGylation affects the deacetylase activity of *SIRT1*. *SIRT1* was purified from *SIRT1* WT- and *SIRT1* KR-complemented *SIRT1* KO cells with or without doxorubicin treatment via immunoprecipitation with an antibody against *SIRT1*. *SIRT1* WT but not *SIRT1* KR was ISGylated upon doxorubicin

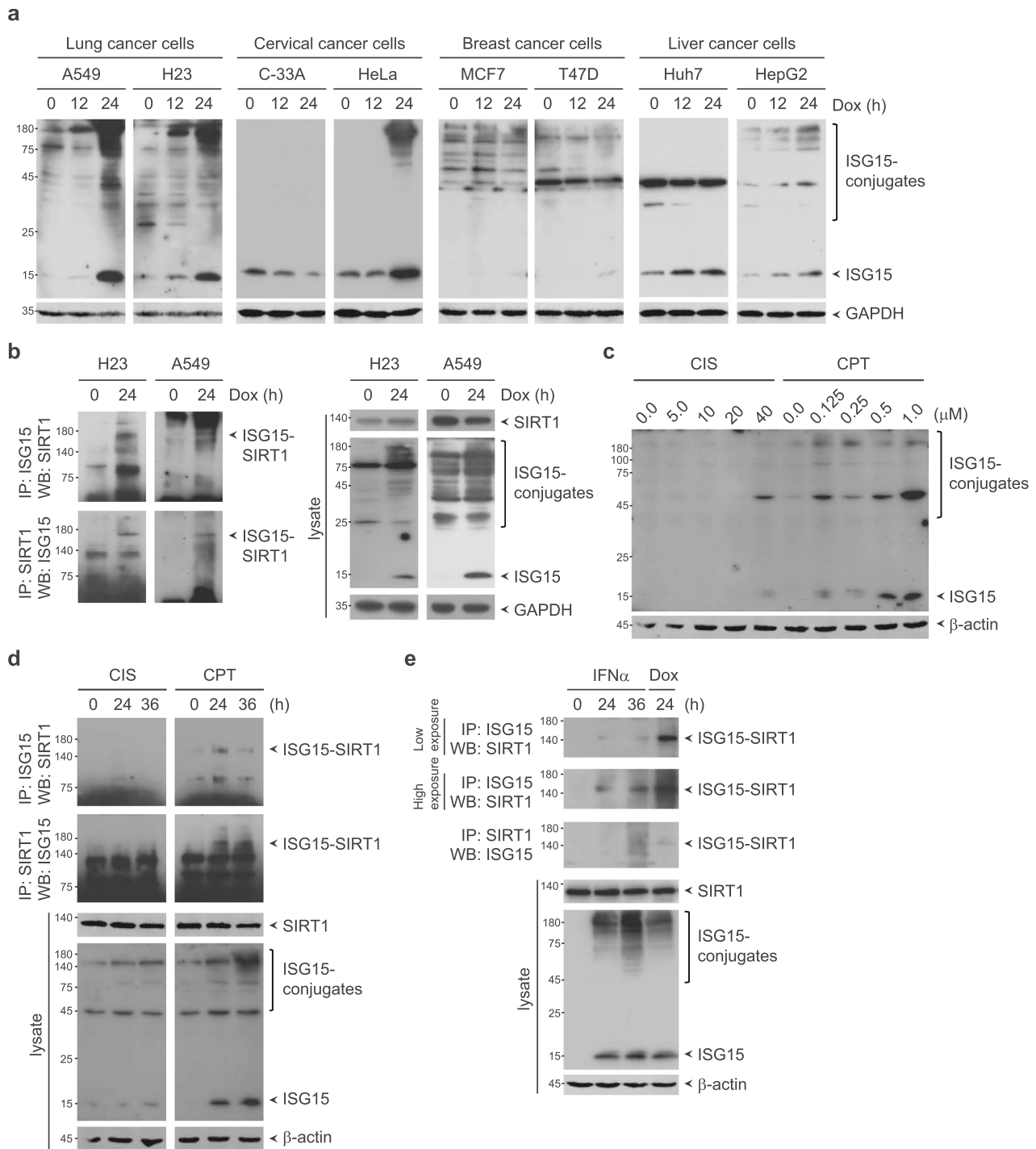
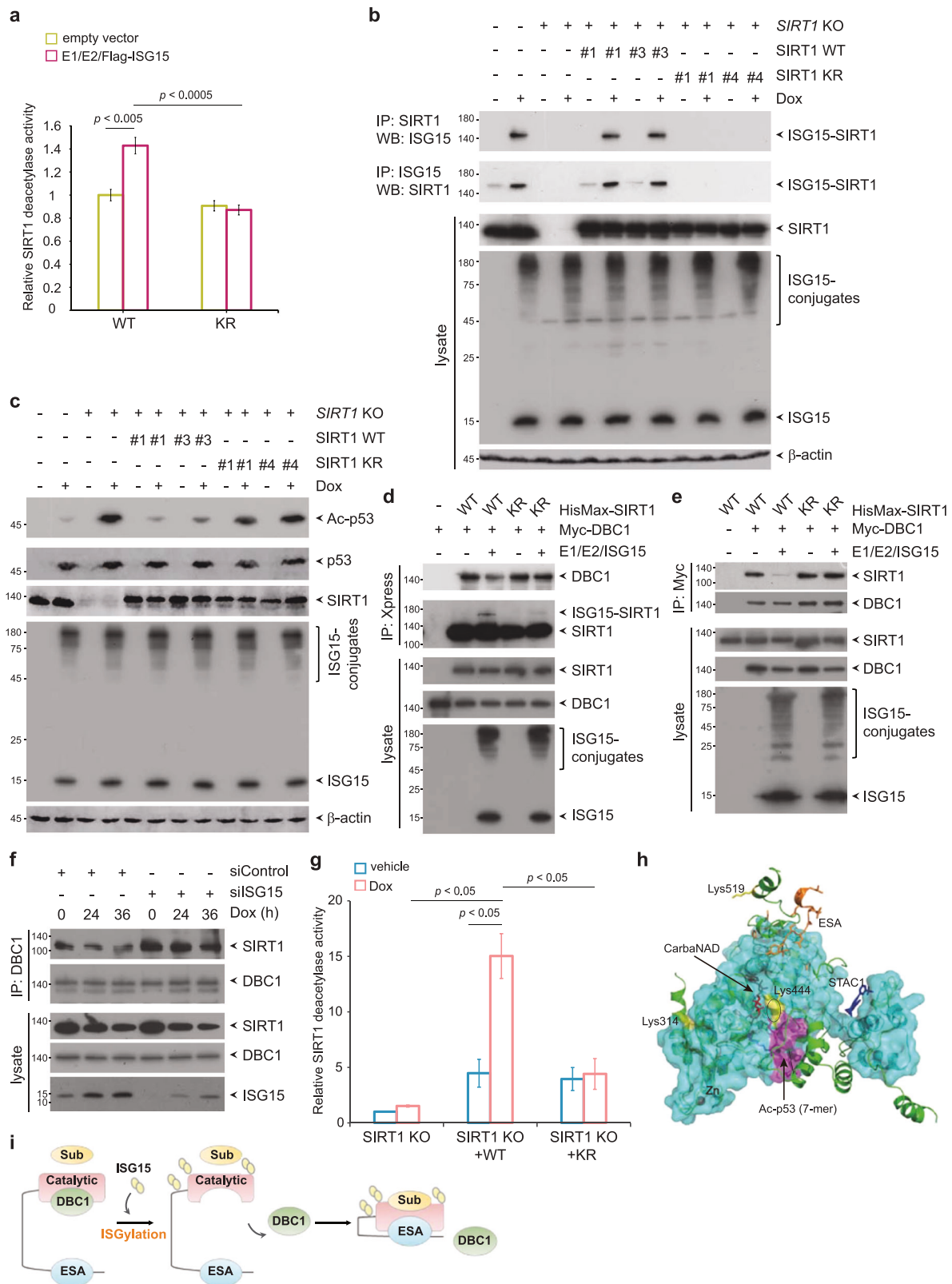


Fig. 3 Induction of SIRT1 ISGylation in response to chemotherapeutic drugs. **a** A549, H23, C-33A, HeLa, MCF7, T47D, Huh7 and HepG2 cells were treated with 0.5 μ M doxorubicin. Cell lysates were subjected to WB analysis with the indicated antibodies. **b** H23 and A549 cells incubated with doxorubicin were subjected to immunoprecipitation (IP) with an anti-ISG15 or anti-SIRT1 antibody followed by WB with an anti-SIRT1 or anti-ISG15 antibody, respectively. **c** A549 cells were incubated with increasing concentrations of cisplatin or camptothecin for 24 h. Cell lysates were subjected to WB analysis with the indicated antibodies. **d** A549 cells were treated with 40 μ M cisplatin or 0.5 μ M camptothecin. Cell lysates were subjected to IP with an anti-ISG15 or anti-SIRT1 antibody followed by WB with an anti-SIRT1 or anti-ISG15 antibody, respectively. **e** A549 cells were treated with 1000 U/ml IFN α or 0.5 μ M doxorubicin. Cell lysates were subjected to IP with an anti-ISG15 or anti-SIRT1 antibody followed by WB with an anti-SIRT1 or anti-ISG15 antibody, respectively.

treatment (Supplementary Fig. 8h). The purified proteins were then subjected to an *in vitro* fluorometric assay to measure their deacetylase activity. As expected, SIRT1 WT showed a significant increase in its deacetylase activity in the presence of doxorubicin compared with in the absence of doxorubicin (Fig. 4g). However,

SIRT1 KR showed no increase in deacetylase activity in the presence of doxorubicin, suggesting that doxorubicin-induced SIRT1 ISGylation significantly increases the deacetylase activity of SIRT1. Active regulator of SIRT1 (AROS), also known as ribosomal protein S19 binding protein 1 (RPS19BP1), interacts with SIRT1 and



amplifies the deacetylation capacity of SIRT1⁶². We therefore examined whether SIRT1 ISGylation regulates the physical interaction between SIRT1 and AROS. AROS and SIRT1 WT or AROS and SIRT1 KR were coexpressed in HEK293T cells in the absence or presence of the ISG15-conjugating system and were reciprocally

coimmunoprecipitated using antibodies directed against V5 or Xpress. SIRT1 ISGylation did not influence the interaction between SIRT1 and AROS (Supplementary Fig. 9).

Analysis of known crystal structures to search for common features of the sequences surrounding the identified ISGylation

Fig. 4 ISGylation of SIRT1 promotes its deacetylase activity. **a** SIRT1 WT and SIRT1 KR in the presence or absence of the ISG15-conjugating system were purified via PD with NTA resin from HEK293T cells and assayed for deacetylase activity using a fluorometric assay system. The bars indicate the mean \pm SD of three independent experiments. **b** Of the many clones (Supplementary Fig. 8e), SIRT1 KO clone #1, SIRT1 KO + WT clones #1 and #3, SIRT1 KO + KR clones #1 and #4, and Control cells were chosen and treated with 1 μ M doxorubicin for 24 h. Cell lysates were subjected to IP with an anti-SIRT1 or anti-ISG15 antibody followed by WB with an anti-ISG15 or anti-SIRT1 antibody, respectively. **c** Lysates of the cells treated as described in (b) were subjected to WB analysis with the indicated antibodies. **d, e** HisMax-tagged SIRT1 WT or SIRT1 KR was transiently coexpressed with Myc-tagged DBC1 with or without the ISG15-conjugating system. Cell lysates were subjected to IP with an anti-Xpress antibody (**d**) or anti-Myc antibody (**e**) followed by WB with an anti-Myc or anti-Xpress antibody, respectively. **f** A549 cells were transfected with siControl or siISG15 and incubated with 0.5 μ M doxorubicin for the indicated times. Cell lysates were subjected to IP with an anti-DBC1 antibody followed by WB with an anti-SIRT1 antibody. **g** SIRT1 was purified via IP with an anti-SIRT1 antibody from SIRT1 KO cells, SIRT1 WT-complemented SIRT1 KO cells and SIRT1 KR-complemented SIRT1 KO cells with or without doxorubicin treatment and assayed for deacetylase activity using a fluorometric assay system. The bars indicate the mean \pm SD of three independent experiments. **h** ISGylation sites in the 3D structure of SIRT1. The structure of mini-hSIRT1 (PDB ID: 4ZZJ) is shown as a ribbon diagram with a transparent cyan surface. The green ribbon represents a model of full-length human SIRT1 generated via AlphaFold but with the structurally inaccurate long loops removed for clarity. The ISGylated lysine residues are depicted as yellow sticks and labeled. The bound cosubstrate analogs carbanicotinamide adenine dinucleotide (CarbANAD) and sirtuin-activating compound (STAC1) are shown as red and blue sticks, respectively. The enzymatic product, the Ac-p53 peptide, is shown as a magenta surface, and the acetylated lysine residue is indicated by an oval. The ESA region in the AlphaFold model is shown in orange. Note that the N-terminal STAC1 binding domain shows different conformations between the experimental and AlphaFold models. **i** A schematic diagram of the regulation of SIRT1 catalytic activity by ISGylation. SIRT1 ISGylation impairs the association of SIRT1 with DBC1, which unleashes SIRT1 from its inactive state and leads to an increase in its deacetylase activity. Furthermore, SIRT1 ISGylation might enhance the intramolecular interaction between the catalytic core domain and the ESA region or increase substrate accessibility.

target Lys residues has suggested that ISGylation occurs at sites associated with protein–protein interactions, in dimerization domains or in enzyme active sites³². Although the 3D structure of full-length mammalian SIRT1 is not yet available, we were able to map the ISGylation sites in the human SIRT1 model based on the partial structure of SIRT1 in complex with a substrate peptide and NAD⁺ analog (Fig. 4h)⁶³. As described above, Lys314 and 444 are in the catalytic domain of SIRT1. In particular, Lys444 is located near the catalytic region where the cosubstrate NAD⁺ and the substrate p53 bind. Lys519 is located in the concealed region outside the catalytic domain toward the C-terminal domain in the experimental structure. Based on the model generated via AlphaFold⁶⁴, we estimated the position of the Lys519 residue, which is relatively close to the essential for SIRT1 activity (ESA) region located in the C-terminus of SIRT1. The intramolecular interaction between the catalytic core domain and the ESA region is essential for the catalytic activity of SIRT1⁶⁵. Therefore, SIRT1 ISGylation might increase the accessibility of substrates or enhance the interaction between the catalytic core domain and the ESA region. Taken together, our findings suggest that SIRT1 ISGylation results in dissociation of the catalytic core domain from DBC1, which unleashes SIRT1 from its inactive state and leads to an increase in its deacetylase activity (Fig. 4i).

SIRT1 ISGylation is required for lung cancer progression and limits sensitivity to DNA damage-based therapeutics

To determine the potential effects of SIRT1 ISGylation on lung cancer progression and therapeutic efficacy, we first examined the impact of SIRT1 ISGylation on lung cancer cell proliferation. We selected clone #1 among the two lentiviral control vector-expressing SIRT1 KO cell lines, clones #1 and #3 among the four SIRT1 WT-complemented SIRT1 KO cell lines, clones #1 and #4 among the four SIRT1 KR-complemented SIRT1 KO cell lines, and Control cells (see Fig. 4b). Doxorubicin significantly induced SIRT1 ISGylation in SIRT1 WT-complemented SIRT1 KO and Control cells but not in SIRT1 KR-complemented SIRT1 KO cells (Supplementary Fig. 10a). Compared with Control cells, SIRT1 KO cells exhibited significant attenuation of cell growth (Fig. 5a). Compared with SIRT1 ablation, complementation of SIRT1 KO cells with either SIRT1 WT or SIRT1 KR facilitated cell growth. Following doxorubicin treatment, compared to SIRT1 ablation, SIRT1 WT complementation significantly attenuated the reduction in cell growth, whereas SIRT1 KR complementation led to only marginal attenuation of the doxorubicin-mediated reduction in cell growth, suggesting the important role of SIRT1 ISGylation in negatively regulating

doxorubicin-mediated inhibition of lung cancer cell proliferation. We next investigated whether SIRT1 ISGylation could be implicated in doxorubicin-induced apoptosis. Doxorubicin treatment of SIRT1 KO cells increased not only the cleavage of poly (ADP-ribose) polymerase (PARP) but also the number of TUNEL-positive apoptotic cells (Fig. 5b, Supplementary Fig. 10b, and Supplementary Fig. 11). Importantly, SIRT1 WT complementation but not SIRT1 KR complementation in SIRT1 KO cells markedly attenuated doxorubicin-induced apoptosis, suggesting that SIRT1 ISGylation negatively regulates doxorubicin-induced apoptosis. Notably, the facilitation of apoptosis in SIRT1 KR-complemented cells upon doxorubicin treatment was mitigated following depletion of DBC1 (Fig. 5c and Supplementary Fig. 12), substantiating the importance of ISGylation-mediated regulation of the association between SIRT1 and DBC1 in controlling doxorubicin-mediated apoptosis. Moreover, compared to SIRT1 ablation, either SIRT1 WT or SIRT1 KR complementation in SIRT1 KO cells led to an increase in the colony formation ability to a level comparable to that of Control cells (Fig. 5d), suggesting the key role of SIRT1 in clonogenic growth. Interestingly, SIRT1 depletion led to a marked decrease in clonogenic growth following doxorubicin treatment. However, compared to SIRT1 KR complementation, SIRT1 WT complementation in SIRT1 KO cells markedly attenuated the doxorubicin-mediated inhibition of clonogenic growth, suggesting that SIRT1 ISGylation is required for lung cancer cell proliferation and survival.

It has been reported that p53 is ISGylated upon DNA damage³³. Upon DNA damage, acetylation and phosphorylation of p53 precede its ISGylation to induce the expression of the ISG15-conjugating system as well as other downstream targets, which leads to further increases in the phosphorylation and acetylation of p53, thereby leading to the suppression of cell growth and tumor development in colorectal carcinoma. To determine whether SIRT1 ISGylation influences p53 ISGylation, SIRT1 WT-complemented and SIRT1 KR-complemented SIRT1 KO cells were treated with doxorubicin for the indicated times. The level of p53 ISGylation increased for 12 h after doxorubicin treatment and remained elevated in SIRT1 WT-complemented and SIRT1 KR-complemented SIRT1 KO cells, even though compared with SIRT1 KR complementation, SIRT1 WT complementation slightly potentiated p53 ISGylation (Fig. 5e). The level of SIRT1 ISGylation in SIRT1 WT-complemented but not in SIRT1 KR-complemented SIRT1 KO cells increased for 12 h after doxorubicin treatment and continued to increase further. SIRT1 ISGylation had little or no effect on p53 phosphorylation. Importantly, immunoblot analysis

Fig. 5 SIRT1 ISGylation plays an essential role in lung cancer cells proliferation and the response of lung cancer cells to DNA-damaging therapeutics. **a** SIRT1 KO clone #1, SIRT1 KO + WT clones #1 and #3, SIRT1 KO + KR clones #1 and #4, and Control cells were treated with 1 μ M doxorubicin for 24 h. Viable cells were counted using trypan blue exclusion. The bars indicate the mean \pm SD of three independent experiments. **b** SIRT1 KO cells, SIRT1 KO cells complemented with SIRT1 WT or SIRT1 KR, and Control cells were incubated with 1 μ M doxorubicin for the indicated times. The cells were then subjected to a TUNEL assay. The number of TUNEL-positive cells was determined and is expressed as a percentage of the total number of cells. The bars indicate the mean \pm SD of three independent experiments. **c** SIRT1 KO cells and SIRT1 WT- or SIRT1 KR-complemented SIRT1 KO cells were transfected with siControl or siDBC1 and incubated with 1 μ M doxorubicin for 24 h. The cells were then subjected to a TUNEL assay. The number of TUNEL-positive cells was determined and is expressed as a percentage of the total number of cells. The bars indicate the mean \pm SD of three independent experiments. **d** SIRT1 KO cells, SIRT1 KO cells complemented with SIRT1 WT or SIRT1 KR, and Control cells were incubated with or without 0.1 μ M doxorubicin for 13 days. Colonies were stained with crystal violet and counted. The bars indicate the mean \pm SD of three independent experiments. **e** SIRT1 WT-complemented and SIRT1 KR-complemented SIRT1 KO cells were treated with 1 μ M doxorubicin for the indicated times. Cell lysates were subjected to IP with an anti-SIRT1 or anti-ISG15 antibody followed by WB with an anti-ISG15 or anti-SIRT1 antibody, respectively, or subjected to IP with an anti-p53 antibody followed by WB with an anti-ISG15 or anti-p53 antibody. Cell lysates were also subjected to WB analysis with the indicated antibodies.

understanding of not only the crosstalk network between SIRT1 ISGylation and p53 ISGylation but also the differential consequences of these processes depending on the tumor context are likely worthwhile.

Based on the above findings that SIRT1 ISGylation promotes cell proliferation and suppresses apoptosis, it is reasonable to postulate that SIRT1 ISGylation plays an important role in lung cancer progression and sensitivity to DNA damage-based therapeutics. To establish the functional role of SIRT1 ISGylation in lung cancer progression and the response to DNA-damaging chemotherapeutics in vivo, we engrafted SIRT1 KO, SIRT1 WT-complemented and SIRT1 KR-complemented cells into BALB/c nude mice. Compared with SIRT1 depletion, SIRT1 WT and SIRT1 KR complementation significantly increased tumor growth in BALB/c nude mice (Fig. 6a, b), substantiating the importance of SIRT1 in driving lung cancer progression. The size of tumors formed from SIRT1 WT-complemented cells in the absence of doxorubicin was greater than that of tumors formed from SIRT1 KR-complemented cells, possibly due to SIRT1 ISGylation resulting from biological events in vivo during tumor development. Intriguingly, SIRT1 WT complementation facilitated tumor growth and rendered tumors resistant to doxorubicin, whereas SIRT1 KR complementation attenuated tumor growth and sensitized tumors to doxorubicin. Taken together, our results suggest that SIRT1 ISGylation promotes lung cancer progression and limits sensitivity to doxorubicin. We sought to validate the ISGylation of SIRT1 in tumors. In accordance with our in vitro study, tumors formed from SIRT1 WT-complemented cells displayed an increase in SIRT1 ISGylation in the presence of doxorubicin compared with that in tumors formed from SIRT1 KR-complemented cells (Fig. 6c).

SIRT1 ISGylation is correlated with poor prognosis in human lung cancer

Prompted by our findings that SIRT1 ISGylation is important for tumor progression and the therapeutic response in lung cancer, we analyzed the protein expression levels of SIRT1 and ISG15 in eleven pairs of primary lung adenocarcinoma tissues and adjacent normal tissues. Higher expression of SIRT1 was found in seven of the lung cancer tissues (63.6%) than in the paired adjacent normal tissues (Fig. 7a). In line with our analyses of the CCLE and TCGA databases (Fig. 2a–c), the protein levels of ISG15 and ISGylation conjugates were high in eight of the lung cancer tissues (72.7%). Interestingly, the levels of not only SIRT1 but also ISG15 and protein ISGylation conjugates were elevated in six of the lung cancer tissues (54.5%), suggesting the involvement of ISG15 and SIRT1 in lung cancer development. The tumor microenvironment is the environment surrounding tumors, where cells continuously recognize danger and damage signals via extracellular and intracellular pattern recognition receptors (PRRs)⁶⁶. One of the important events is type I IFN production and the subsequent upregulation of ISG15 and its related enzymes during cancer development, supporting our findings of elevated ISG15 expression and ISGylation in lung cancer tissues² and

suggesting that the upregulation of ISG15 expression and ISGylation is directly or indirectly linked to the pathogenesis of cancer.

To further extend our observations to a clinicopathologically relevant context, we analyzed the protein expression levels of SIRT1 and ISG15 in NSCLC patients-derived lung cancer tissues. After dual-immunohistochemical staining (IHC), SIRT1 was visible as brown staining and ISG15 as red staining (Fig. 7b). Based on the IHC staining scores (Supplementary Fig. 13), the lung cancer tissues were subdivided into high- and low-expression groups. According to these cutoff values, no clinicopathologic factor was significantly associated with the combined expression of SIRT1 and ISG15 (SIRT1/ISG15) or with the individual expression of SIRT1 or ISG15 (Supplementary Table 1). High SIRT1 expression (SIRT1^{hi} (log rank $P = 0.028$)) and high ISG15 expression (ISG15^{hi} (log rank $P = 0.022$)) were each significantly associated with a decrease in overall survival in NSCLC patients (Fig. 7c, d). Importantly, high combined expression of SIRT1 and ISG15 (SIRT1^{hi}/ISG15^{hi} (log-rank $P < 0.001$)) was positively correlated with poor prognosis in NSCLC patients (Fig. 7e). Given that patients with lung adenocarcinoma had a 3.206-fold greater risk of death (95% CI: 1.293–7.947) than patients with squamous cell lung carcinoma, we performed an additional analysis to evaluate the prognostic significance of SIRT1, ISG15, and SIRT1/ISG15 expression in patients with squamous cell lung carcinoma and lung adenocarcinoma. SIRT1^{hi} (log rank $P = 0.018$) was associated with decreased overall survival in squamous cell lung carcinoma patients (Fig. 7f). Intriguingly, SIRT1^{hi}/ISG15^{hi} was significantly correlated with poor prognosis in not only squamous cell lung carcinoma patients (log rank $P = 0.012$) (Fig. 7g) but also lung adenocarcinoma patients (log rank $P < 0.001$) (Fig. 7h). In univariate analysis, the expression status of SIRT1, ISG15, or SIRT1/ISG15 was identified as a factor strongly associated with overall survival (Supplementary Table 2). The SIRT1^{hi}/ISG15^{hi} phenotype was associated with a 3.477-fold greater risk of death and poor survival (95% confidence interval (95% CI); 1.685–7.176, $P < 0.001$) in lung cancer patients compared with the SIRT1^{lo}/ISG15^{lo} phenotype. According to our multivariate analysis, the SIRT1^{hi}/ISG15^{hi} phenotype was an independent indicator of a shorter survival time in lung cancer patients (Supplementary Table 3). The SIRT1^{hi}/ISG15^{hi} phenotype was associated with a 4.984-fold greater risk of death (95% CI: 2.175–11.423, $P < 0.001$) in patients. Taken together, our results revealed that elevated expression levels of SIRT1 and ISG15 are associated with the progressive phenotype of lung cancer and are positively correlated with poor prognosis in lung cancer patients, suggesting that ISG15 and SIRT1 are prognostic indicators in human lung cancer.

DISCUSSION

In response to both extracellular and intracellular perturbations, SIRT1 is tightly regulated by alterations in its expression, associations with other proteins, and posttranslational modifications (PTMs), which can ultimately govern physiological and

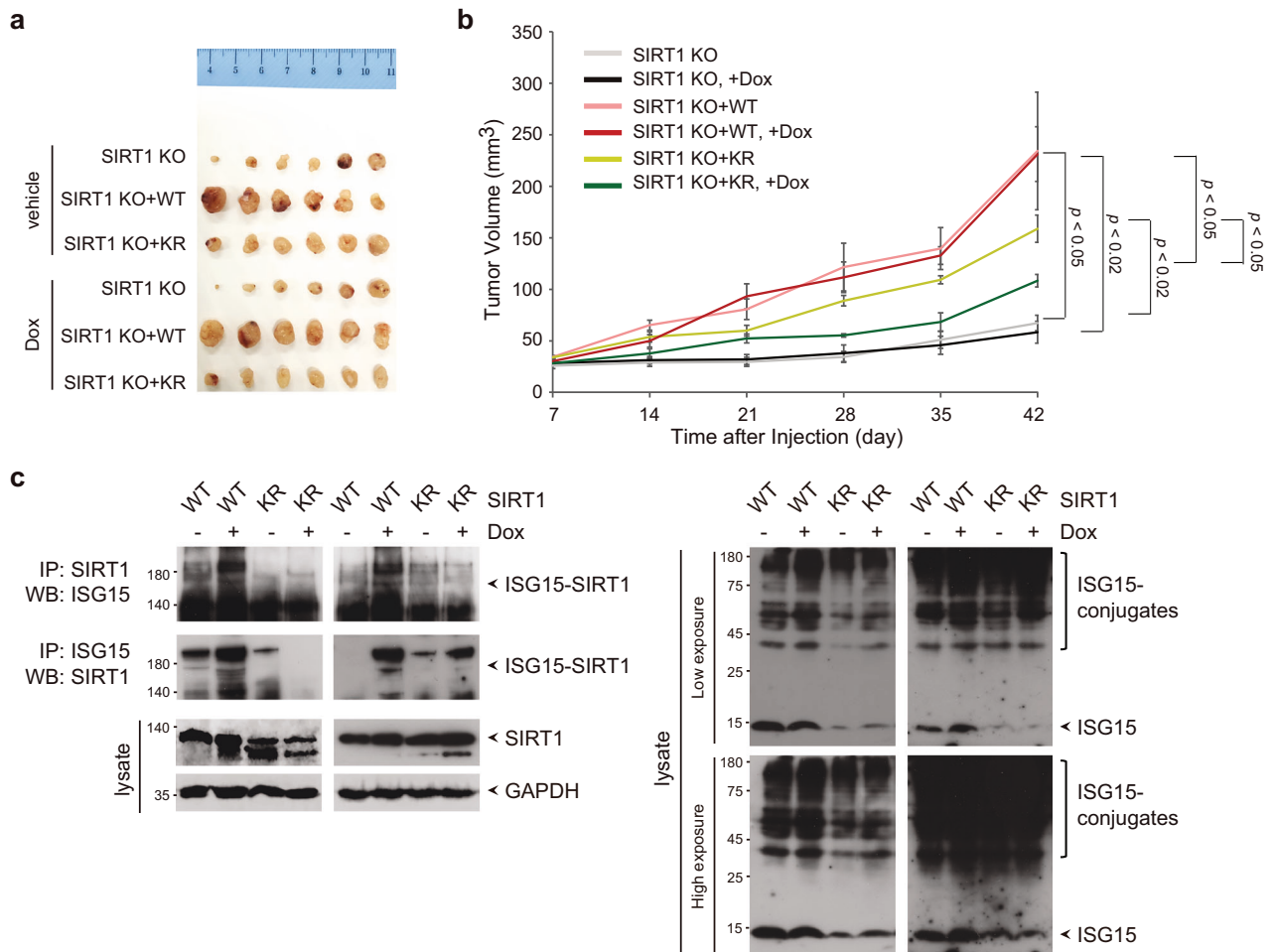


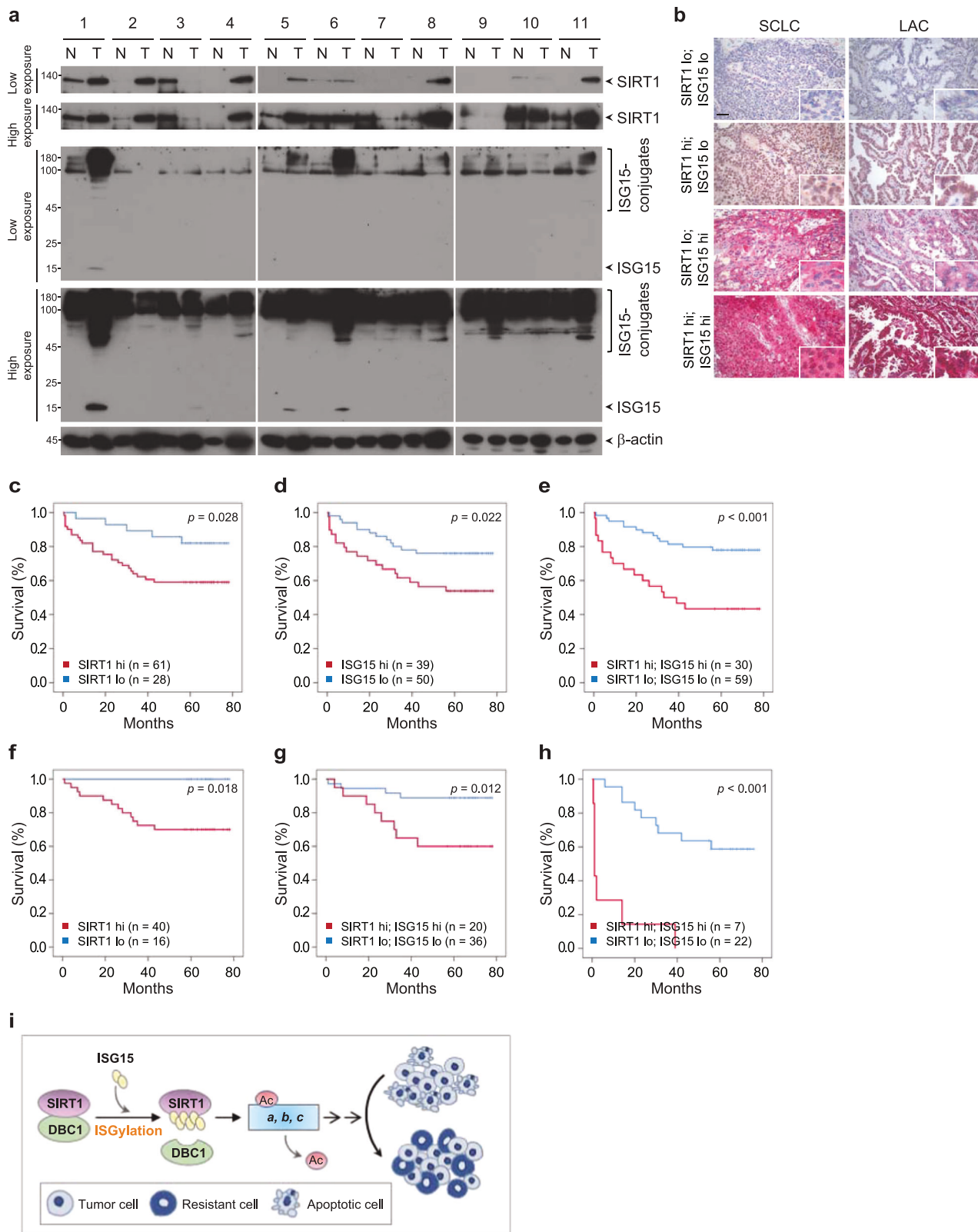
Fig. 6 SIRT1 ISGylation limits tumor responses to doxorubicin. a, b SIRT1 KO cells and SIRT1 KO cells complemented with SIRT1 WT or SIRT1 KR were injected into BALB/c nude mice, and the mice were monitored weekly for tumor growth. The animals were subjected to doxorubicin treatment 4 days after injection, as described in the Methods section. The mice were sacrificed, and tumors were harvested (**a**). The bars indicate the means \pm SEMs. $n = 6$ mice per treatment group (**b**). **c** Tumors formed as described in (**a**) were lysed and subjected to IP with an anti-SIRT1 or anti-ISG15 antibody followed by WB with an anti-ISG15 or anti-SIRT1 antibody, respectively. The lysates were also directly probed with the indicated antibodies.

pathophysiological processes and diseases. Although SIRT1 has been studied in cancer research in recent decades, the role of SIRT1 in cancer has remained controversial, likely due to the genetic background of cancer, type of tissue, stage of cancer, and distinct regulation of SIRT1, which might differentially affect substrates. Our current work reveals a novel molecular mechanism underlying SIRT1 ISGylation for the regulation of tumor progression and the response to DNA-damaging chemotherapeutics in lung cancer, as depicted in the summary schematic (Fig. 7i).

We showed that SIRT1 ISGylation induced by treatment with the DNA-damaging chemotherapeutic agent doxorubicin impairs the interaction of SIRT1 with DBC1, which unleashes SIRT1 from its inactive state and leads to an increase in its deacetylase activity. Although the structure for the complex between SIRT1 and DBC1 has not been determined, the ESA region located in the C-terminus of SIRT1 has been shown to compete with DBC1 to interact with the catalytic core domain⁶⁵. Based on the ISGylation sites in SIRT1, we speculate that ISGylation at Lys444 might be involved in the dissociation of DBC1 to expose the substrate binding site. The functional consequence of ISGylation at Lys314 has not been determined. However, we are tempted to speculate that ISGylation at Lys314 induces a conformational change to a closed state, because the zinc-binding and helical modules in the catalytic domain move upon binding of the cosubstrate NAD⁺ and a

substrate⁶⁷. Additionally, it is possible that Lys519 may participate in strengthening the binding of the ESA to the catalytic core. However, the exact structural changes in SIRT1 caused by ISGylation need to be further explored via structural studies.

PTMs can occur very rapidly in cells and are highly dynamic to accommodate constantly changing signals in the cells. In addition to single regulatory PTMs, there are also PTMs that function in orchestrated manners. The combinatorial action of multiple PTMs on the same protein or different proteins is termed PTM crosstalk^{68,69}. It is possible that ISGylation of SIRT1 might occur in concert or compete with multiple PTMs of SIRT1, thereby driving cumulative outputs to modulate the catalytic activity, binding affinity for substrate proteins, stability, and subcellular localization of SIRT1. The N- and C-terminal regulatory domains of SIRT1 are targets of numerous PTMs, including phosphorylation, SUMOylation, glycosylation, and S-glutathionylation^{70–72}. SIRT1 is SUMOylated at a lysine residue in the C-terminus, preserving its deacetylase activity, which permits SIRT1 to inhibit the transcription of apoptosis-related genes⁷³. PTMs in the catalytic core domain of SIRT1 have begun to be identified. Recently, phosphorylation, S-nitrosylation, and carbonylation have been demonstrated to regulate SIRT1^{74–80}. SIRT1 was shown to be ubiquitinated in the catalytic core domain, which decreases its stability^{81,82}. Therefore, future studies to explore how one dynamic



PTM can affect another PTM in the same or a neighboring domain and how the mechanisms of crosstalk between PTMs can result in coordinated control of the activity of SIRT1 are likely worthwhile.

SIRT1 ISGylation promotes not only tumorigenesis but also chemoresistance in vivo and in vitro models of lung cancer. Lung

cancer is the most fatal cancer worldwide, mainly because of the rapid emergence of intrinsic and acquired chemoresistance, adaptive oncogenic mutations, and poor prognosis⁸³. Although several pathological parameters, including tumor-positive lymph node status and tumor size, have been suggested to have

Fig. 7 SIRT1 ISGylation serves as a prognostic marker in human NSCLCs. **a** Tumor tissues and the paired adjacent normal tissues derived from 11 lung adenocarcinoma patients were lysed and subjected to WB with the indicated antibodies. **b** Representative immunostaining of squamous cell lung carcinomas (SCLCs) and lung adenocarcinomas (LACs) depicting high and low levels of SIRT1 and ISG15 expression. SIRT1 staining appears brown, and ISG15 staining appears red. Original magnification, 400x. Scale bar = 50 μ m. Kaplan–Meier curves comparing the OS of lung cancer patients with tumors expressing high or low levels of SIRT1 ($P = 0.028$) (**c**), high or low levels of ISG15 ($P = 0.022$) (**d**), or high or low levels of SIRT1 combined with high or low levels of ISG15 ($P < 0.001$) (**e**). **f**, **g** Kaplan–Meier curves comparing the survival of squamous cell lung carcinoma patients with tumors expressing high or low levels of SIRT1 ($P = 0.018$) (**f**) and high or low levels of SIRT1 combined with high or low levels of ISG15 ($P = 0.012$) (**g**). **h** Kaplan–Meier curve comparing the survival of adenocarcinoma patients with tumors expressing high or low levels of SIRT1 combined with high or low levels of ISG15 ($P < 0.001$). **i** A schematic model showing a novel molecular mechanism through which SIRT1 ISGylation controls tumor progression and sensitivity to DNA damage-based therapeutics in lung cancer. SIRT1 ISGylation impairs the association of SIRT1 with DBC1, thereby potentiating the enzymatic activity of SIRT1, which promotes tumorigenesis and limits the sensitivity of lung cancer to DNA damage-based therapeutics.

prognostic value in lung cancer patients, there are still limitations in predicting lung cancer progression, recurrence, and drug resistance. From the perspective of clinical relevance, we revealed that SIRT1 and ISG15 were upregulated in primary lung adenocarcinoma tissues from lung cancer patients compared to the corresponding adjacent normal tissues. Furthermore, elevated expression of SIRT1 and ISG15 in NSCLC tumors was strongly associated with poor prognosis, suggesting that SIRT1 ISGylation is of potential prognostic value in NSCLC patients. Elevated expression of SIRT1 in human NSCLCs is positively associated with advanced tumor stage, metastasis, and worse prognosis^{84–86}. Importantly, SIRT1 upregulation is positively correlated with both a reduction in apoptosis and resistance to chemotherapeutic drugs, including doxorubicin, in various types of cancer and in cancer stem cells^{87–91}. SIRT1 inhibition enhances the antitumor activity of MK-1775 in lung cancer⁴⁹. Furthermore, SIRT1 is a potential predictor of poor prognosis in NSCLC patients treated with platinum-based chemotherapy, and SIRT1 downregulation greatly increases chemosensitivity to cisplatin, indicating the important role of SIRT1 in driving lung cancer development and chemoresistance. Therefore, our findings pave the way for understanding the regulatory mechanism of SIRT1 in cancer cell fate decisions. Moreover, our preliminary transcriptional profiles generated by RNA-Seq of cells derived from lung cancer with or without doxorubicin suggested that SIRT1 could be positively correlated with the expression of genes in key pathways associated with the propensity for cancer development and resistance to various therapies, including the mitogen-activated protein kinase (MAPK), phosphoinositide 3-kinase (PI3K)-protein kinase B (AKT), Ras, Janus kinase/signal transducer and activator of transcription (JAK-STAT), and nuclear factor kappa-light-chain-enhancer of activated B cells (NF- κ B) signaling pathways (unpublished data). Further in-depth investigations of the transcriptomic features coordinated by SIRT1 and SIRT1 ISGylation might be geared toward not only understanding the contributions of SIRT1 and SIRT1 ISGylation to cancer cell proliferation and apoptosis but also identifying feasible biomarkers for therapeutic responsiveness.

Lysine acetylation is one of the most important PTMs and broadly regulates diverse sets of cellular functions. Therefore, understanding the dynamics of lysine acetylation is essential for deciphering its functions in the regulation of physiological processes and dysregulated or disease states. We are currently attempting to determine how changes in the lysine acetylome are regulated by SIRT1 ISGylation and to delineate the mechanism through which acetylome dynamics are implicated in tumorigenesis and the therapeutic response.

ISG15 has emerged as an important regulator of diverse cellular processes, including metabolic reprogramming, the immune response, the DNA damage response, autophagy, exosome secretion, cytoskeletal dynamics, and telomere shortening^{2,31,32,53,92–96}. However, studies on the functions of ISG15 in cancer pathogenesis and therapeutic responsiveness have generated many conflicting results that indicate its context-dependent tumor-promoting or tumor-suppressive activity. Here, our current

work highlights the importance of ISGylation in orchestrating lung cancer progression and limiting sensitivity to DNA damage-inducing therapy. This mechanism is highly consistent with the results in our in vivo model and clinical outcomes. Unlike the comparable protein levels of ISG15 and ISGylation conjugates between clonal cell lines (Fig. 4b), significant induction of protein ISGylation conjugates formation but only marginal induction of the expression of free ISG15 was observed in tumors in the presence of doxorubicin, potentially because of biological events occurring in vivo (Fig. 6c). Interestingly, the protein levels of ISG15 and/or ISGylation conjugates in tumors formed from SIRT1 WT-complemented cells were higher than those in tumors formed from SIRT1 KR-complemented cells in either the absence or presence of doxorubicin, which might explain why the tumors formed from SIRT1 WT-complemented cells in the absence of doxorubicin were larger than the tumors formed from SIRT1 KR-complemented cells, suggesting the necessity of further investigation of the relationship between SIRT1 ISGylation and the induction of ISG15 expression and protein ISGylation conjugates formation in vivo. Another question is why our in vivo findings did not precisely mirror our in vitro findings. ISG15 and protein ISGylation conjugates affect the physiological states of tumors in a manner dependent on internal and external stimuli and orchestrate tumor–tumor microenvironment communication during cancer development, resulting in tumor progression or tumor suppression⁹⁷. These complex biological responses might result from the pleiotropic actions of ISG15 and ISGylation as well as various feedback control mechanisms, which appear to be dependent on the tumor context and tumor microenvironment. Therefore, we cannot rule out the possibility that the induction of ISG15 expression and protein ISGylation conjugates formation in lung tumors modulates the tumor environment, suggesting the necessity of further investigation of the role of ISG15 and ISGylation in the regulation of tumor–tumor microenvironment communication and the coordination of tumor responses to therapies.

Chemo- and radiotherapy are designed to eliminate cancer cells by inducing DNA damage exceeding the capacity of the DNA damage response⁹⁸. However, cancer cells often exhibit abnormalities in the DNA damage response, rendering them resistant to DNA damage-based therapy⁹⁹. In addition, even though cancer patients initially exhibit favorable responses to the widely used chemotherapeutic drug doxorubicin, the majority of cancer patients experience undesirable side effects and exhibit intrinsic or acquired resistance. *ISG15* is an IFN-related DNA damage resistance signature (IRDS) gene⁵⁶. The IRDS is a signature indicating resistance to DNA-damaging therapies, suggesting that information about the IRDS status significantly improves outcome prediction when combined with standard markers, risk group stratification, or other genomic classifiers. Importantly, ISG15 has been demonstrated to promote resistance to DNA-damaging chemo- and radiotherapy in different cancer types and to be correlated with unfavorable prognosis¹⁰⁰, suggesting the potential of targeting ISG15 for resensitization of tumor cells and

improvement of the outcome of anticancer therapy. Overall, we envisage that targeting SIRT1 ISGylation could amplify the antitumor effects of DNA damage-based therapies in the treatment of lung cancer.

Supplementary information

The supplementary information is provided in a PDF file. The supplementary information for this article is available at <https://www.nature.com/emm> and accompanies the manuscript on the Experimental & Molecular Medicine website (<https://www.nature.com/emm>).

DATA AVAILABILITY

The data generated or analyzed during this study are included in this published article and its supplementary data files. All relevant data supporting the present study are available from the corresponding author upon reasonable request.

REFERENCES

- Haas, A. L., Ahrens, P., Bright, P. M. & Ankel, H. Interferon induces a 15-kilodalton protein exhibiting marked homology to ubiquitin. *J. Biol. Chem.* **262**, 11315–11323 (1987).
- Han, H. G., Moon, H. W. & Jeon, Y. J. ISG15 in cancer: beyond ubiquitin-like protein. *Cancer Lett.* **438**, 52–62 (2018).
- Desai, S. D. et al. ISG15 disrupts cytoskeletal architecture and promotes motility in human breast cancer cells. *Exp. Biol. Med.* **237**, 38–49 (2012).
- Yang, H. et al. Hrd1-mediated BLIMP-1 ubiquitination promotes dendritic cell MHCII expression for CD4 T cell priming during inflammation. *J. Exp. Med.* **211**, 2467–2479 (2014).
- Hermann, M.-R. et al. Integrins synergise to induce expression of the MRTF-A-SRF target gene ISG15 for promoting cancer cell invasion. *J. Cell Sci.* **129**, 1391–1403 (2016).
- Sainz, B., Martin, B., Tatari, M., Heeschen, C. & Guerra, S. ISG15 is a critical microenvironmental factor for pancreatic cancer stem cells. *Cancer Res.* **74**, 7309–7320 (2014).
- Sun, J. et al. Loss of TRIM29 suppresses cancer stem cell-like characteristics of PDACs via accelerating ISG15 degradation. *Oncogene* **39**, 546–559 (2019).
- Fan, J.-B. et al. Type I interferon regulates a coordinated gene network to enhance cytotoxic T cell-mediated tumor killing. *Cancer Discov.* **10**, 382–393 (2020).
- Bogunovic, D. et al. Mycobacterial disease and impaired IFN- γ immunity in humans with inherited ISG15 deficiency. *Science* **337**, 1684–1688 (2012).
- Okumura, A., Pitha, P. M. & Harty, R. N. ISG15 inhibits Ebola VP40 VLP budding in an L-domain-dependent manner by blocking Nedd4 ligase activity. *Proc. Natl. Acad. Sci. USA* **105**, 3974–3979 (2008).
- Swaim, C. D., Scott, A. F., Canadeo, L. A. & Huibregtse, J. M. Extracellular ISG15 signals cytokine secretion through the LFA-1 integrin receptor. *Mol. Cell* **68**, 581–590. e585 (2017).
- Yuan, W. & Krug, R. M. Influenza B virus NS1 protein inhibits conjugation of the interferon (IFN)-induced ubiquitin-like ISG15 protein. *Embo J.* **20**, 362–371 (2001).
- Zhao, C. et al. The UbcH8 ubiquitin E2 enzyme is also the E2 enzyme for ISG15, an IFN- α /beta-induced ubiquitin-like protein. *Proc. Natl. Acad. Sci. USA* **101**, 7578–7582 (2004).
- Kim, K. I., Giannakopoulos, N. V., Virgin, H. W. & Zhang, D. E. Interferon-inducible ubiquitin E2, Ubc8, is a conjugating enzyme for protein ISGylation. *Mol. Cell. Biol.* **24**, 9592–9600 (2004).
- Okumura, F., Zou, W. & Zhang, D. E. ISG15 modification of the eIF4E cognate 4EHP enhances cap structure-binding activity of 4EHP. *Genes Dev.* **21**, 255–260 (2007).
- Tan, N. G. et al. Human homologue of Ariadne promotes the ubiquitylation of translation initiation factor 4E homologous protein, 4EHP. *FEBS Lett.* **554**, 501–504 (2003).
- Zou, W. & Zhang, D. E. The interferon-inducible ubiquitin-protein isopeptide ligase (E3) EFP also functions as an ISG15 E3 ligase. *J. Biol. Chem.* **281**, 3989–3994 (2006).
- Dastur, A., Beaudenon, S., Kelley, M., Krug, R. M. & Huibregtse, J. M. Herc5, an interferon-induced HECT E3 enzyme, is required for conjugation of ISG15 in human cells. *J. Biol. Chem.* **281**, 4334–4338 (2006).
- Wong, J. J., Pung, Y. F., Sze, N. S. & Chin, K. C. HERC5 is an IFN-induced HECT-type E3 protein ligase that mediates type I IFN-induced ISGylation of protein targets. *Proc. Natl. Acad. Sci. USA* **103**, 10735–10740 (2006).
- Ketscher, L., Basters, A., Prinz, M. & Knobeloch, K.-P. mHERC6 is the essential ISG15 E3 ligase in the murine system. *Biochem. Biophys. Res. Commun.* **417**, 135–140 (2012).
- Malakhov, M. P., Malakhova, O. A., Kim, K. I., Ritchie, K. J. & Zhang, D. E. UBP43 (USP18) specifically removes ISG15 from conjugated proteins. *J. Biol. Chem.* **277**, 9976–9981 (2002).
- Basters, A. et al. Structural basis of the specificity of USP18 toward ISG15. *Nat. Struct. Mol. Biol.* **24**, 270–278 (2017).
- Jeon, Y. J. et al. Chemosensitivity is controlled by p63 modification with ubiquitin-like protein ISG15. *J. Clin. Invest.* **122**, 2622–2636 (2012).
- Ochi, K. et al. Prediction of response to neoadjuvant chemotherapy for osteosarcoma by gene-expression profiles. *Int. J. Oncol.* **24**, 647–655 (2004).
- Park, J. M. et al. Modification of PCNA by ISG15 plays a crucial role in termination of error-prone translesion DNA synthesis. *Mol. Cell* **54**, 626–638 (2014).
- Pitha-Rowe, I., Petty, W., Kitareewan, S. & Dmitrovsky, E. Retinoid target genes in acute promyelocytic leukemia. *Leukemia* **17**, 1723–1730 (2003).
- Kang, J. A., Kim, Y. J. & Jeon, Y. J. The diverse repertoire of ISG15: More intricate than initially thought. *Exp. Mol. Med.* **54**, 1779–1792 (2022).
- Giannakopoulos, N. V. et al. Proteomic identification of proteins conjugated to ISG15 in mouse and human cells. *Biochem. Biophys. Res. Commun.* **336**, 496–506 (2005).
- Zhao, C., Denison, C., Huibregtse, J. M., Gygi, S. & Krug, R. M. Human ISG15 conjugation targets both IFN-induced and constitutively expressed proteins functioning in diverse cellular pathways. *Proc. Natl. Acad. Sci. USA* **102**, 10200–10205 (2005).
- Malakhov, M. P. et al. High-throughput immunoblotting: ubiquitin-like protein ISG15 modifies key regulators of signal transduction. *J. Biol. Chem.* **278**, 16608–16613 (2003).
- Yan, S. et al. IRF3 reduces adipose thermogenesis via ISG15-mediated reprogramming of glycolysis. *J. Clin. Invest.* **131**, e144888 (2021).
- Zhang, Y. et al. The in vivo ISGylome links ISG15 to metabolic pathways and autophagy upon *Listeria monocytogenes* infection. *Nat. Commun.* **10**, 1–15 (2019).
- Park, J. H. et al. Positive feedback regulation of p53 transactivity by DNA damage-induced ISG15 modification. *Nat. Commun.* **7**, 12513 (2016).
- Imai, S.-I., Armstrong, C. M., Kaeberlein, M. & Guarente, L. Transcriptional silencing and longevity protein Sir2 is an NAD-dependent histone deacetylase. *Nature* **403**, 795–800 (2000).
- Liu, T., Liu, P. Y. & Marshall, G. M. The critical role of the class III histone deacetylase SIRT1 in cancer. *Cancer Res.* **69**, 1702–1705 (2009).
- Raynes, R., Brunquell, J. & Westerheide, S. D. Stress inducibility of SIRT1 and its role in cytoprotection and cancer. *Genes Cancer* **4**, 172–182 (2013).
- Kaushal, P., Kwon, Y., Ju, S. & Lee, C. An SDS-PAGE based proteomic approach for N-terminome profiling. *Analyst* **144**, 7001–7009 (2019).
- Lee, S. et al. tipNrich: a tip-based N-terminal proteome enrichment method. *Anal. Chem.* **93**, 14088–14098 (2021).
- Brademan, D. R., Riley, N. M., Kwiecien, N. W. & Coon, J. J. Interactive peptide spectral annotator: a versatile web-based tool for proteomic applications. *Mol. Cell. Proteom.* **18**, S193–S201 (2019).
- Hussein, U. K. et al. Expression of oxidized protein tyrosine phosphatase and γ H2AX predicts poor survival of gastric carcinoma patients. *BMC Cancer* **18**, 1–12 (2018).
- Park, H. J. et al. The PARP inhibitor olaparib potentiates the effect of the DNA damaging agent doxorubicin in osteosarcoma. *J. Exp. Clin. Cancer Res.* **37**, 1–15 (2018).
- Nusinow, D. P. et al. Quantitative proteomics of the cancer cell line encyclopedia. *Cell* **180**, 387–402 (2020).
- Ghandi, M. et al. Next-generation characterization of the cancer cell line encyclopedia. *Nature* **569**, 503–508 (2019).
- Padovan, E. et al. Interferon stimulated gene 15 constitutively produced by melanoma cells induces E-cadherin expression on human dendritic cells. *Cancer Res.* **62**, 3453–3458 (2002).
- Burks, J., Reed, R. & Desai, S. ISGylation governs the oncogenic function of Ki-Ras in breast cancer. *Oncogene* **33**, 794–803 (2014).
- Chen, Y.-L. et al. Interferon-stimulated gene 15 modulates cell migration by interacting with Rac1 and contributes to lymph node metastasis of oral squamous cell carcinoma cells. *Oncogene* **38**, 4480–4495 (2019).
- Bektas, N. et al. The ubiquitin-like molecule interferon-stimulated gene 15 (ISG15) is a potential prognostic marker in human breast cancer. *Breast Cancer Res.* **10**, 1–12 (2008).
- Cruz, A. C. T. & Mejía-Barreto, K. Cell type-dependent regulation of free ISG15 levels and ISGylation. *J. Cell Commun. Signal* **11**, 127–135 (2017).
- Chen, G. et al. Suppression of Sirt1 sensitizes lung cancer cells to WEE1 inhibitor MK-1775-induced DNA damage and apoptosis. *Oncogene* **36**, 6863–6872 (2017).
- Liu, M., Hummer, B. T., Li, X. & Hassel, B. A. Camptothecin induces the ubiquitin-like protein, ISG15, and enhances ISG15 conjugation in response to interferon. *J. Interferon Cytokine Res.* **24**, 647–654 (2004).
- Zitvogel, L., Galluzzi, L., Kepp, O., Smyth, M. J. & Kroemer, G. Type I interferons in anticancer immunity. *Nat. Rev. Immunol.* **15**, 405–414 (2015).
- Benci, J. L. et al. Tumor interferon signaling regulates a multigenic resistance program to immune checkpoint blockade. *Cell* **167**, 1540–1554 (2016).

53. Yeh, Y.-H., Yang, Y.-C., Hsieh, M.-Y., Yeh, Y.-C. & Li, T.-K. A negative feedback of the HIF-1 α pathway via interferon-stimulated gene 15 and ISGylation. *Clin. Cancer Res.* **19**, 5927–5939 (2013).
54. Levy, D. E. & Gilliland, D. G. Divergent roles of STAT1 and STAT5 in malignancy as revealed by gene disruptions in mice. *Oncogene* **19**, 2505–2510 (2000).
55. Borden, E., Hogan, T. & Voelkel, J. Comparative antiproliferative activity in vitro of natural interferons α and β for diploid and transformed human cells. *Cancer Res.* **42**, 4948–4953 (1982).
56. Weichselbaum, R. R. et al. An interferon-related gene signature for DNA damage resistance is a predictive marker for chemotherapy and radiation for breast cancer. *Proc. Natl. Acad. Sci. USA* **105**, 18490–18495 (2008).
57. Erdal, E., Haider, S., Rehwinkel, J., Harris, A. L. & McHugh, P. J. A prosurvival DNA damage-induced cytoplasmic interferon response is mediated by end resection factors and is limited by Trex1. *Genes Dev.* **31**, 353–369 (2017).
58. Jeon, Y. J. et al. ISG15 modification of filamin B negatively regulates the type I interferon-induced JNK signalling pathway. *EMBO Rep.* **10**, 374–380 (2009).
59. Im, E., Yoo, L., Hyun, M., Shin, W. H. & Chung, K. C. Covalent ISG15 conjugation positively regulates the ubiquitin E3 ligase activity of parkin. *Open Biol.* **6**, 160193 (2016).
60. Kim, J.-E., Chen, J. & Lou, Z. DBC1 is a negative regulator of SIRT1. *Nature* **451**, 583 (2008).
61. Zhao, W. et al. Negative regulation of the deacetylase SIRT1 by DBC1. *Nature* **451**, 587 (2008).
62. Kim, E.-J., Kho, J.-H., Kang, M.-R. & Um, S.-J. Active regulator of SIRT1 cooperates with SIRT1 and facilitates suppression of p53 activity. *Mol. Cell* **28**, 277–290 (2007).
63. Dai, H. et al. Crystallographic structure of a small molecule SIRT1 activator-enzyme complex. *Nat. Commun.* **6**, 1–10 (2015).
64. Jumper, J. et al. Highly accurate protein structure prediction with AlphaFold. *Nature* **596**, 583–589 (2021).
65. Kang, H. et al. Peptide switch is essential for Sirt1 deacetylase activity. *Mol. Cell* **44**, 203–213 (2011).
66. Patel, S. A. & Minn, A. J. Combination cancer therapy with immune checkpoint blockade: mechanisms and strategies. *Immunity* **48**, 417–433 (2018).
67. Davenport, A. M., Huber, F. M. & Hoelz, A. Structural and functional analysis of human SIRT1. *J. Mol. Biol.* **426**, 526–541 (2014).
68. Dai Vu, L., Gevaert, K. & De Smet, I. Protein language: post-translational modifications talking to each other. *Trends Plant Sci.* **23**, 1068–1080 (2018).
69. Leutert, M., Entwistle, S. W. & Villén, J. Decoding post-translational modification crosstalk with proteomics. *Mol. Cell. Proteom.* **20**, 100129 (2021).
70. Lee, C.-W. et al. AMPK promotes p53 acetylation via phosphorylation and inactivation of SIRT1 in liver cancer cells. *Cancer Res.* **72**, 4394–4404 (2012).
71. Chattopadhyay, T. et al. Spatiotemporal gating of SIRT1 functions by O-GlcNAcylation is essential for liver metabolic switching and prevents hyperglycemia. *Proc. Natl. Acad. Sci. USA* **117**, 6890–6900 (2020).
72. Zee, R. S. et al. Redox regulation of sirtuin-1 by S-glutathiolation. *Antioxid. Redox Signal.* **13**, 1023–1032 (2010).
73. Yang, Y. et al. SIRT1 sumoylation regulates its deacetylase activity and cellular response to genotoxic stress. *Nat. Cell Biol.* **9**, 1253–1262 (2007).
74. Wang, W. et al. JAK1-mediated Sirt1 phosphorylation functions as a negative feedback of the JAK1-STAT3 pathway. *J. Biol. Chem.* **293**, 11067–11075 (2018).
75. Lau, A. W., Liu, P., Inuzuka, H. & Gao, D. SIRT1 phosphorylation by AMP-activated protein kinase regulates p53 acetylation. *Am. J. Cancer Res.* **4**, 245–255 (2014).
76. Gerhart-Hines, Z. et al. The cAMP/PKA pathway rapidly activates SIRT1 to promote fatty acid oxidation independently of changes in NAD⁺. *Mol. Cell* **44**, 851–863 (2011).
77. Kalous, K. S., Wynia-Smith, S. L., Summers, S. B. & Smith, B. C. Human sirtuins are differentially sensitive to inhibition by nitrosating agents and other cysteine oxidants. *J. Biol. Chem.* **295**, 8524–8536 (2020).
78. Kalous, K. S., Wynia-Smith, S. L., Olp, M. D. & Smith, B. C. Mechanism of Sirt1 NAD⁺-dependent protein deacetylase inhibition by cysteine S-nitrosation. *J. Biol. Chem.* **291**, 25398–25410 (2016).
79. Kornberg, M. D. et al. GAPDH mediates nitrosylation of nuclear proteins. *Nat. Cell Biol.* **12**, 1094–1100 (2010).
80. Caito, S. et al. SIRT1 is a redox-sensitive deacetylase that is post-translationally modified by oxidants and carbonyl stress. *FASEB J.* **24**, 3145–3159 (2010).
81. Lin, Z. et al. USP22 antagonizes p53 transcriptional activation by deubiquitinating Sirt1 to suppress cell apoptosis and is required for mouse embryonic development. *Mol. Cell* **46**, 484–494 (2012).
82. Peng, L. et al. Ubiquitinated sirtuin 1 (SIRT1) function is modulated during DNA damage-induced cell death and survival. *J. Biol. Chem.* **290**, 8904–8912 (2015).
83. Torre, L. A., Siegel, R. L. & Jemal, A. Lung cancer statistics. *Lung Cancer Pers. Med.* **893**, 1–19 (2016).
84. Chen, X. et al. Sirt1 is a tumor promoter in lung adenocarcinoma. *Oncol. Lett.* **8**, 387–393 (2014).
85. Grbesa, I. et al. Expression of sirtuin 1 and 2 is associated with poor prognosis in non-small cell lung cancer patients. *PLoS One* **10**, e0124670 (2015).
86. Wang, J. & Wang, C. Prognostic and predictive role of Sirtuin1 expression in lung adenocarcinoma. *Clin. Lab.* **62**, 1989–1994 (2016).
87. Jin, X. et al. High expression of SIRT1 associates with the doxorubicin resistance of breast cancer through the activation of Akt. *Anti Cancer Agents Med. Chem.* **20**, 94–102 (2020).
88. Wei, T., Xiaojun, X. & Peilong, C. Magnoflorine improves sensitivity to doxorubicin (DOX) of breast cancer cells via inducing apoptosis and autophagy through AKT/mTOR and p38 signaling pathways. *Biomed. Pharmacother.* **121**, 109139 (2020).
89. Xu, M. et al. CPEB1 mediates hepatocellular carcinoma cancer stemness and chemoresistance. *Cell Death Dis.* **9**, 1–17 (2018).
90. Chen, J. et al. Sirtuin 1 is upregulated in a subset of hepatocellular carcinomas where it is essential for telomere maintenance and tumor cell growth. *Cancer Res.* **71**, 4138–4149 (2011).
91. Song, S. et al. Protective effects of dioscin against doxorubicin-induced hepatotoxicity via regulation of Sirt1/FOXO1/NF- κ B signal. *Front. Pharmacol.* **10**, 1030 (2019).
92. Villarroya-Beltri, C. et al. ISGylation controls exosome secretion by promoting lysosomal degradation of MVB proteins. *Nat. Commun.* **7**, 1–11 (2016).
93. Raso, M. C. et al. Interferon-stimulated gene 15 accelerates replication fork progression inducing chromosomal breakage. *J. Cell Biol.* **219**, e202002175 (2020).
94. Xu, D. et al. Modification of BECN1 by ISG15 plays a crucial role in autophagy regulation by type I IFN/interferon. *Autophagy* **11**, 617–628 (2015).
95. Kang, J. A. & Jeon, Y. J. Emerging roles of USP18: from biology to pathophysiology. *Int. J. Mol. Sci.* **21**, 6825 (2020).
96. Alcalá, S. et al. ISG15 and ISGylation is required for pancreatic cancer stem cell mitophagy and metabolic plasticity. *Nat. Commun.* **11**, 1–17 (2020).
97. Stark, G. R. & Darnell, J. E. Jr. The JAK-STAT pathway at twenty. *Immunity* **36**, 503–514 (2012).
98. Ummat, A. et al. Structural basis for cisplatin DNA damage tolerance by human polymerase η during cancer chemotherapy. *Nat. Struct. Mol. Biol.* **19**, 628–632 (2012).
99. Wang, B., Hurov, K., Hofmann, K. & Elledge, S. J. NBA1, a new player in the Brca1 A complex, is required for DNA damage resistance and checkpoint control. *Genes Dev.* **23**, 729–739 (2009).
100. Wood, L. M., Pan, Z.-K., Seavey, M. M., Muthukumaran, G. & Paterson, Y. The ubiquitin-like protein, ISG15, is a novel tumor-associated antigen for cancer immunotherapy. *Cancer Immunol. Immunother.* **61**, 689–700 (2012).

ACKNOWLEDGEMENTS

This work was supported by National Research Foundation of Korea (NRF) grants from the Korean government (NRF-2019R1A2C2002324 to Y.J.J. and NRF-2022M3H9A2096187 to C.L.). J.A.K. was the recipient of the BK21 Plus fellowship.

AUTHOR CONTRIBUTIONS

Y.J.K. and J.A.K. performed most of the experiments; Y.S.Y., H.W.M., and H.G.H. conducted parts of the experiments; S.W.C. and C.Y.C. generated the A549 cells depleted of SIRT1 by CRISPR–Cas9 genome editing with specific guide RNAs (gRNAs); G.M.H., C.C., M.J.C., and K.Y.J. analyzed data and performed pathological analyses of lung cancer patients; H.L., M.K., and Y.K. performed bioinformatics analyses with the CCLE and TCGA databases; S.L. and C.L. performed ISGylation sites mapping by mass spectrometry; H.K.S. performed structural analysis of ISGylation sites in SIRT1; Y.J.J. designed the experiments, analyzed the data, supervised the entire project, wrote the manuscript, and oversaw generation of the reagents.

COMPETING INTERESTS

The authors declare no competing interests.

ADDITIONAL INFORMATION

Supplementary information The online version contains supplementary material available at <https://doi.org/10.1038/s12276-024-01194-2>.

Correspondence and requests for materials should be addressed to Young Joo Jeon.

Reprints and permission information is available at <http://www.nature.com/reprints>

Publisher's note Springer Nature remains neutral with regard to jurisdictional claims in published maps and institutional affiliations.



Open Access This article is licensed under a Creative Commons Attribution 4.0 International License, which permits use, sharing, adaptation, distribution and reproduction in any medium or format, as long as you give appropriate credit to the original author(s) and the source, provide a link to the Creative Commons licence, and indicate if changes were made. The images or other third party material in this article are included in the article's Creative Commons licence, unless indicated otherwise in a credit line to the material. If material is not included in the article's Creative Commons licence and your intended use is not permitted by statutory regulation or exceeds the permitted use, you will need to obtain permission directly from the copyright holder. To view a copy of this licence, visit <http://creativecommons.org/licenses/by/4.0/>.

© The Author(s) 2024